3

EFFECTIVE PROPAGATION CONSTANTS IN MEDIA WITH DENSELY DISTRIBUTED DIELECTRIC PARTICLES OF MULTIPLE SIZES AND PERMITTIVITIES

K. H. Ding and L. Tsang

3.1 Introduction

In a dense medium, the particles occupy an appreciable fractional volume. In a nontenuous medium, the dielectric properties of the particles are substantially different from that of the background medium. In recent years, studies of the propagation and scattering of waves in dense nontenuous media have been made with applications to geophysical terrain and composite materials [1–9]. Such media often consist of mixtures of particles with multiple sizes and permittivities that are embedded in a background medium. It has been shown both theoretically and experimentally that in a dense nontenuous medium, the assumption that the particles scatter independently is not valid. A more rigorous theory is needed to take into account correlated scattering between particles.

In section 3.2, we outline the governing multiple scattering equations for random discrete scatterers. Various approximations to calculate the first moment of the field are discussed. The treatment includes the important case of dense nontenuous medium with multiple species of particles. The multiple species refers to the fact that the medium is a mixture of particles with different sizes and permittivities. Special emphases are placed on the Quasicrystalline Approximation (QCA) and the Quasicrystalline Approximation with Coherent Potential (QCA–CP) [2,8].

In section 3.3, the pair distribution function is discussed. Specifically, the Percus–Yevick approximation is used to calculate the pair distribution functions in a medium with non-interpenetrable spheres of multiple sizes [10–16]. Numerical results of pair distribution functions are illustrated as functions of particle sizes and fractional volumes.

In section 3.4, the low frequency limit of the dispersion relations under the QCA and QCA–CP approximations is considered. Analytic closed form expressions are obtained for the complex effective propagation constants. Numerical results are illustrated as functions of particle sizes, fractional volumes, and dielectric properties.

In section 3.5, we consider the case of moderate size particles. The QCA equations are formulated in terms of the T-matrix formulism and utilizing vector spherical waves as basis functions [4,8]. The final equations of the dispersion relation for multi-species are solved numerically and illustrated as functions of the physical properties of the particles.

In section 3.6, we examine energy conservation. In multiple scattering problems of lossless media or slightly lossy media, one key objec-

tive is to calculate the second moment and the incoherent intensity of waves [17,18]. For these problems, the calculation of the first moment and the effective propagation constant serves as an intermediate step. Thus, approximation of the first moment must be done with due regard to energy conservation and consistency with the second moment. It is shown in section 3.6 that QCA–CP is energetically consistent with the ladder approximation of second moment. This is analogous to the nonlinear approximation of continuous random medium theory [19]. The QCA–CP has been used in conjunction with the ladder approximation modified with the pair distribution function to derive a set of dense medium radiative transfer equations that obey energy conservation and include multiple scattering of the incoherent fields [8,20–22]. In section 3.6, we also derive the intensity operator under ladder approximation of correlated scatterers for multiple species which will be useful for second moment calculations and which also obeys energy conservation.

The problem of multiple particle sizes and permittivities is an important one for both geophysical terrain and composite materials. The particles in natural geophysical terrain are usually not of identical sizes. They usually follow a drop size distribution which can be discretized and represented by a histogram. Thus, the approach given in this paper for the calculation of effective propagation constants for such cases of random discrete scatterers of multiple sizes gives a better description of the effects of correlated scattering.

3.2 Multiple Scattering Equations and Dispersion Relations

Consider a random medium consisting of N discrete scatterers of L different species, located at $\overline{r}_1, \overline{r}_2, \ldots, \overline{r}_N$ in a volume V of background medium with permittivity ϵ (Fig. 3.2.1). The different species refer to the fact that particles can be of different shapes, sizes, and permittivities. However, interpenetration of particles is not allowed. The different species are denoted by $s_j = 1, 2, \ldots, L$. Each species of particles can have a distinct size, shape, and permittivity ϵ_{s_j}.

To study the propagation of electromagnetic waves in such a medium, a multiple scattering theory based on dyadic Green's operator can be applied. The N-particle dyadic Green's operator $\overline{\overline{G}}$ satisfies

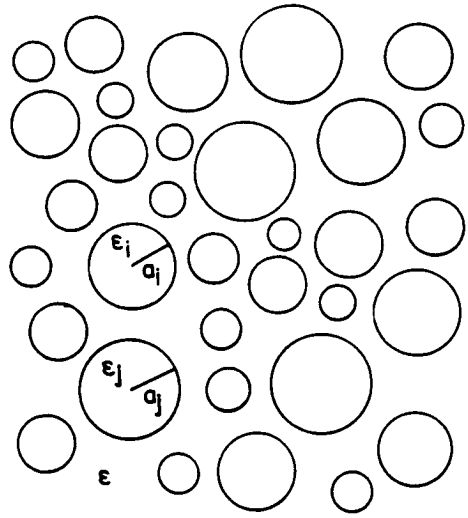

Figure 3.2.1 Discrete nontenuous media with multi-species particles with different sizes and permittivities.

the multiple scattering equations [2,8]

$$\overline{\overline{G}} = \overline{\overline{G}}_o + \overline{\overline{G}}_o \sum_{j=1}^{N} \overline{\overline{U}}_j^{s_j} \overline{\overline{G}} \tag{1}$$

where $\overline{\overline{G}}_o$ is the dyadic Green's operator of the background medium with propagation constant $k = \omega\sqrt{\mu\epsilon}$, ω is the angular frequency, and μ is the permeability. The scattering potential operator, $\overline{\overline{U}}_j^{s_j}$, associated with the j th scatterer of species s_j is such that

$$\begin{aligned} \left\langle \overline{r} \mid \overline{\overline{U}}_j^{s_j} \mid \overline{r}' \right\rangle &= U^{s_j}(\overline{r} - \overline{r}_j)\,\overline{\overline{I}}\,\delta(\overline{r} - \overline{r}') \\ &= U_j^{s_j}(\overline{r})\,\overline{\overline{I}}\,\delta(\overline{r} - \overline{r}') \end{aligned} \tag{2}$$

where $\overline{\overline{I}}$ is unit dyad and

$$U^{s_j}(\overline{r} - \overline{r}_j) = \begin{cases} 0 & \text{for } \overline{r} \text{ outside particle } j \\ k_{s_j}^2 - k^2 & \text{for } \overline{r} \text{ inside particle } j \end{cases} \tag{3}$$

with $k_{s_j} = \omega\sqrt{\mu\epsilon_{s_j}}$ being the wavenumber in the s_j type scatterers.

The particle distribution is described by the many-particle probability density function $p(\bar{r}_1, \bar{r}_2, \ldots, \bar{r}_N; s_1, s_2, \ldots, s_L)$. The first and second order statistics are given by

$$Np(\bar{r}_i; s_i) = n_{s_i} \tag{4}$$

$$(N-1)p(\bar{r}_j; s_j \mid \bar{r}_i; s_i) = n_{s_j} g_{s_i s_j}(\bar{r}_i, \bar{r}_j) \tag{5}$$

where $p(\mid)$ is the conditional probability function, n_{s_i} is the number density of s_i type particles, and $g_{s_i s_j}(\bar{r}_i, \bar{r}_j)$ is the pair distribution functions for two particles of species s_i and s_j. Using Bayes rule, it follows readily that $g_{s_i s_j}$ is symmetric so that $g_{s_i s_j}(\bar{r}_i, \bar{r}_j) = g_{s_j s_i}(\bar{r}_j, \bar{r}_i)$.

Generally, the Green's function in (1) depends on the locations and types of the N particles. The concept of configuration average [8] is used to obtain the average Green's function as a function of number densities and pair distribution functions. Quasicrystalline Approximation (QCA) and Quasicrystalline Approximation with Coherent Potential (QCA–CP) are applied to derive the dispersion relations and the results are obtained in the momentum representations.

a. Quasicrystalline Approximation (QCA)

Given the scattering potential operator $\overline{\overline{U}}_j^{s_j}$ for the j th scatterer of s_j species, the transition operator $\overline{\overline{T}}_j^{s_j}$ associated with this particle satisfies the Lippmann–Schwinger equation

$$\overline{\overline{T}}_j^{s_j} = \overline{\overline{U}}_j^{s_j} + \overline{\overline{U}}_j^{s_j} \overline{\overline{G}}_o \overline{\overline{T}}_j^{s_j} \tag{6}$$

which describes the scattering of wave from the j th particle in the absence of all other particles. In terms of this single particle transition operator $\overline{\overline{T}}_j^{s_j}$, a scattering operator $\overline{\overline{Q}}_j^{s_j}$ at $\bar{r}_j$ is defined as [8]

$$\overline{\overline{Q}}_j^{s_j} = \overline{\overline{T}}_j^{s_j} + \overline{\overline{T}}_j^{s_j} \overline{\overline{G}}_o \sum_{l \neq j}^{N} \overline{\overline{Q}}_l^{s_l} \tag{7}$$

which can be interpreted as scattering operator for the j th particle in the presence of other particles. In terms of $\overline{\overline{Q}}_j^{s_j}$, the multiple scattering equation (1) becomes

$$\overline{\overline{G}} = \overline{\overline{G}}_o + \overline{\overline{G}}_o \sum_{j=1}^{N} \overline{\overline{Q}}_j^{s_j} \overline{\overline{G}}_o \tag{8}$$

The configuration average of $\overline{\overline{G}}$ and $\overline{\overline{Q}}_j^{sj}$ are

$$E\left(\overline{\overline{G}}\right) = \overline{\overline{G}}_o + N\overline{\overline{G}}_o E\left[E_j\left(\overline{\overline{Q}}_j^{sj}\right)\right]\overline{\overline{G}}_o \tag{9}$$

$$E_l\left(\overline{\overline{Q}}_l^{sl}\right) = \overline{\overline{T}}_l^{sl} + (N-1)\overline{\overline{T}}_l^{sl}\overline{\overline{G}}_o E_l\left[E_{lj}\left(\overline{\overline{Q}}_j^{sj}\right)\right] \tag{10}$$

where E stands for the expectation value, E_j is the conditional average given the position and species of particle j, and E_{lj} is the conditional average of given the positions and species of particles j and l. Thus,

$$E\left[E_j\left(\overline{\overline{Q}}_j^{sj}\right)\right] = \iint d\bar{r}_j ds_j p(\bar{r}_j; s_j) E_j\left(\overline{\overline{Q}}_j^{sj}\right) \tag{11}$$

$$E_l\left[E_{lj}\left(\overline{\overline{Q}}_j^{sj}\right)\right] = \iint d\bar{r}_j ds_j p(\bar{r}_j; s_j \mid \bar{r}_l; s_l) E_{lj}\left(\overline{\overline{Q}}_j^{sj}\right) \tag{12}$$

Equations (9) and (10) indicate that the total average is given in terms of the conditional average with one particle fixed and the conditional average with one particle fixed is given in terms of the conditional average with two particles fixed. In a similar manner, we can express the conditional average with n particles fixed in terms of the conditional average with $n+1$ particles fixed. A hierarchy of equations is thus generated. Truncation at various stages leads to different approximations.

Under quasicrystalline approximation, truncation is made at the second stage of the hierarchy of equations

$$E_{lj}\left(\overline{\overline{Q}}_j^{sj}\right) \approx E_j\left(\overline{\overline{Q}}_j^{sj}\right) \tag{13}$$

Assuming discrete values of s_j, we can replace the integration with respect to s_j in (11) and (12) by the summation over s_j. From the properties of (4) and (5), $E\left(\overline{\overline{G}}\right)$ and $E_l\left(\overline{\overline{Q}}_l^{sl}\right)$ can be expressed as

$$E\left(\overline{\overline{G}}\right) = \overline{\overline{G}}_o + \overline{\overline{G}}_o \sum_{s_j=1}^{L} n_{s_j} \int d\bar{r}_j E_j\left(\overline{\overline{Q}}_j^{sj}\right)\overline{\overline{G}}_o \tag{14}$$

$$E_l\left(\overline{\overline{Q}}_l^{sl}\right) = \overline{\overline{T}}_l^{sl} + \overline{\overline{T}}_l^{sl}\overline{\overline{G}}_o \sum_{s_j=1}^{L} n_{s_j} \int d\bar{r}_j g_{s_l s_j}(\bar{r}_l, \bar{r}_j) E_j\left(\overline{\overline{Q}}_j^{sj}\right) \tag{15}$$

Assume the solution for $E_l\left(\overline{\overline{Q}}_l^{s_l}\right)$ in the momentum representation as [8]

$$\left\langle \bar{p} \mid E_l\left(\overline{\overline{Q}}_l^{s_l}\right) \mid \bar{p}' \right\rangle = e^{-i(\bar{p}-\bar{p}')\cdot\bar{r}_l}\, \overline{\overline{Q}}_p^{s_l}(\bar{p},\bar{p}') \tag{16}$$

Further let

$$\overline{\overline{C}}_p^{s_l}(\bar{p},\bar{p}') = \overline{\overline{Q}}_p^{s_l}(\bar{p},\bar{p}') \left[\bar{\bar{I}} + \overline{\overline{G}}_o(\bar{p}') \sum_{s_j=1}^{L} n_{s_j} \overline{\overline{Q}}_p^{s_j}(\bar{p}',\bar{p}')\right]^{-1} \tag{17}$$

The quantity $\overline{\overline{C}}_p^{s_l}(\bar{p},\bar{p}')$ is governed by an integral equation as follows

$$\overline{\overline{C}}_p^{s_l}(\bar{p},\bar{p}') = \overline{\overline{T}}_p^{s_l}(\bar{p},\bar{p}') + \sum_{s_j=1}^{L} n_{s_j} \times \int d\bar{p}'' \overline{\overline{T}}_p^{s_l}(\bar{p},\bar{p}'')$$
$$\overline{\overline{G}}_o(\bar{p}'')\, H_{s_l s_j}(\bar{p}''-\bar{p}')\, \overline{\overline{C}}_p^{s_j}(\bar{p}'',\bar{p}') \tag{18}$$

where $H_{s_l s_j}(\bar{p})$ is defined as

$$H_{s_l s_j}(\bar{p}) = \frac{1}{(2\pi)^3} \int d\bar{r} h_{s_l s_j}(\bar{r}) \exp(-i\bar{p}\cdot\bar{r}) \tag{19}$$

and

$$h_{s_l s_j}(\bar{r}) = g_{s_l s_j}(\bar{r}) - 1 \tag{20}$$

and $\overline{\overline{T}}_p^{s_j}(\bar{p},\bar{p}') = \left\langle \bar{p} \mid \overline{\overline{T}}^{s_j} \mid \bar{p}' \right\rangle$ is the momentum representation of $\overline{\overline{T}}^{s_j}$. For statistical homogeneous medium, the average dyadic Green's operator is diagonal in the momentum representation, $\left\langle \bar{p} \mid E\left(\overline{\overline{G}}\right) \mid \bar{p}' \right\rangle = \overline{\overline{G}}(\bar{p}) \langle \bar{p} \mid \bar{p}' \rangle$, and $\overline{\overline{G}}(\bar{p})$ is given by

$$\overline{\overline{G}}(\bar{p}) = \left[\overline{\overline{G}}_o^{-1}(\bar{p}) - \sum_{s_j=1}^{L} n_{s_j} \overline{\overline{C}}_p^{s_j}(\bar{p},\bar{p})\right]^{-1} \tag{21}$$

where $\overline{\overline{C}}_p^{s_j}(\bar{p},\bar{p}')$ satisfies the integral equation (18). By setting the determinant of the inverse of $\overline{\overline{G}}(\bar{p})$ equals to zero, the dispersion relation is obtained as

$$\det\left[\overline{\overline{G}}_o^{-1}(\bar{p}) - \sum_{s_j=1}^{L} n_{s_j} \overline{\overline{C}}_p^{s_j}(\bar{p},\bar{p})\right] = 0 \tag{22}$$

where det stands for determinant. The complex value of $\bar{p}$ given by solution of (22) is the effective propagation constant K. Thus, the equations of QCA for multiple species consist of solving (18) for $\overline{\overline{C}}_p^{s_j}(\bar{p},\bar{p}')$ and then substituting that in (22) to calculate the effective propagation constant K.

The dispersion equations of (18) and (22) can also be expressed in terms of mass operator. We define the operator $\overline{\overline{C}}_j^{s_j}$ that is a function of $\bar{r}_j$ and s_j such that

$$\left\langle \bar{p} \mid \overline{\overline{C}}_j^{s_j} \mid \bar{p}' \right\rangle = e^{-i(\bar{p}-\bar{p}')\cdot\bar{r}_j}\, \overline{\overline{C}}_p^{s_j}(\bar{p},\bar{p}') \tag{23}$$

Equation (18) can be put in operator form

$$\overline{\overline{C}}_l^{s_l} = \overline{\overline{T}}_l^{s_l} + \sum_{s_j=1}^{L} n_{s_j} \int d\bar{r}_j h_{s_l s_j}(\bar{r}_j - \bar{r}_l)\, \overline{\overline{T}}_l^{s_l}\, \overline{\overline{G}}_o\, \overline{\overline{C}}_j^{s_j} \tag{24}$$

Thus, $\overline{\overline{C}}_l^{s_l}$ can be interpreted as the scattering transition operator of particle l in the presence of other particles averaged over particle positions and properties under the QCA approximation. The operator equation equivalent to (21) is then

$$E\left(\overline{\overline{G}}\right) = \overline{\overline{G}}_o + \overline{\overline{G}}_o \sum_{s_j=1}^{L} n_{s_j} \int d\bar{r}_j\, \overline{\overline{C}}_j^{s_j} E\left(\overline{\overline{G}}\right) \tag{25}$$

Let

$$\overline{\overline{M}} = \sum_{s_j=1}^{L} n_{s_j} \int d\bar{r}_j\, \overline{\overline{C}}_j^{s_j} \tag{26}$$

be the dyadic mass operator for the medium with scatterers of L different species under the quasicrystalline approximation. Equation (25) can be rewritten as

$$E\left(\overline{\overline{G}}\right) = \overline{\overline{G}}_o + \overline{\overline{G}}_o \overline{\overline{M}} E\left(\overline{\overline{G}}\right) \tag{27}$$

In terms of the mass operator, the dispersion relation of (21) becomes

$$\overline{\overline{G}}(\bar{p}) = \left[\overline{\overline{G}}_o^{-1}(\bar{p}) - \overline{\overline{M}}(\bar{p},\bar{p})\right]^{-1} \tag{28}$$

with

$$\left\langle \bar{p} \mid \overline{\overline{M}} \mid \bar{p}' \right\rangle = \langle \bar{p} \mid \bar{p}' \rangle \sum_{s_j=1}^{L} n_{s_j} \overline{\overline{C}}_p^{s_j}(\bar{p}, \bar{p}) \tag{29}$$

b. Quasicrystalline Approximation with Coherent Potential (QCA-CP)

In the coherent potential approximation [8,23–26], the medium is described by a coherent potential operator $\overline{\overline{w}}(\bar{p})$ which is constant in space but may be a function of the momentum operator $\bar{p}$. By adding and subtracting an operator $n\overline{\overline{w}}(\bar{p})$, (1) can be expressed as

$$\overline{\overline{G}} = \left[\overline{\overline{G}}_o^{-1} - n\overline{\overline{w}}(\bar{p}) - \sum_{j=1}^{N} \left(\overline{\overline{U}}_j^{s_j} - \frac{\overline{\overline{w}}(\bar{p})}{V} \right) \right]^{-1} \tag{30}$$

where

$$n = \sum_{s_j=1}^{L} n_{s_j} \tag{31}$$

is the total number density of particles. Let $\overline{\overline{G}}_c^{-1} = \overline{\overline{G}}_o^{-1} - n\overline{\overline{w}}(\bar{p})$ be the the coherent potential Green's operator and $\tilde{\overline{\overline{U}}}_j^{s_j} = \overline{\overline{U}}_j^{s_j} - \overline{\overline{w}}(\bar{p})/V$ be the modified potential operator. In terms of $\overline{\overline{G}}_c$ and $\tilde{\overline{\overline{U}}}_j^{s_j}$, the multiple scattering equation (1) becomes

$$\overline{\overline{G}} = \overline{\overline{G}}_c + \overline{\overline{G}}_c \sum_{j=1}^{N} \tilde{\overline{\overline{U}}}_j^{s_j} \overline{\overline{G}} \tag{32}$$

The QCA–CP approximation is introduced by applying QCA to the scattering equation of (32) with the new potential $\tilde{\overline{\overline{U}}}_j^{s_j}$ and then imposing the self-consistent condition that the average Green's operator must be the same as the coherent potential Green's operator i.e. $E\left(\overline{\overline{G}}\right) = \overline{\overline{G}}_c$. With the $\overline{\overline{G}}_o$ in equation (6) replaced by $\overline{\overline{G}}_c$, a modified transition operator $\tilde{\overline{\overline{t}}}_j^{s_j}$ is defined to satisfy

$$\tilde{\overline{\overline{t}}}_j^{s_j} = \overline{\overline{U}}_j^{s_j} + \overline{\overline{U}}_j^{s_j} \overline{\overline{G}}_c \tilde{\overline{\overline{t}}}_j^{s_j} \tag{33}$$

The result for the average Green's operator under QCA becomes

$$\overline{\overline{G}}(\bar{p}) = \overline{\overline{G}}_c(\bar{p}) = \left[\overline{\overline{G}}_o^{-1}(\bar{p}) - \sum_{s_j=1}^{L} n_{s_j} \overline{\overline{\hat{C}}}_p^{s_j}(\bar{p},\bar{p})\right]^{-1} \tag{34}$$

where $\overline{\overline{\hat{C}}}_p^{s_j}(\bar{p},\bar{p}')$ satisfies the integral equation

$$\overline{\overline{\hat{C}}}_p^{s_l}(\bar{p},\bar{p}') = \overline{\overline{\hat{t}}}_p^{s_l}(\bar{p},\bar{p}') + \sum_{s_j=1}^{L} n_{s_j} \times \int d\bar{p}'' \overline{\overline{\hat{t}}}_p^{s_l}(\bar{p},\bar{p}'') \overline{\overline{G}}_c(\bar{p}'') H_{s_l s_j}(\bar{p}'' - \bar{p}') \overline{\overline{\hat{C}}}_p^{s_j}(\bar{p}'',\bar{p}') \tag{35}$$

and $\overline{\overline{\hat{t}}}_p^{s_j}(\bar{p},\bar{p}') = \left\langle \bar{p} \left| \overline{\overline{\hat{t}}}^{s_j} \right| \bar{p}' \right\rangle$ is the momentum representation of $\overline{\overline{\hat{t}}}^{s_j}$. The dispersion relation for QCA–CP is

$$\det\left[\overline{\overline{G}}_o^{-1}(\bar{p}) - \sum_{s_j=1}^{L} n_{s_j} \overline{\overline{\hat{C}}}_p^{s_j}(\bar{p},\bar{p})\right] = 0 \tag{36}$$

Thus solution of QCA–CP is provided by first solving (32) and (34). Substituting $\overline{\overline{\hat{C}}}_p^{s_j}(\bar{p},\bar{p}')$ in (35) and solving for $\bar{p}$ gives the complex effective propagation constant K.

Similarly, the dispersion relations of (35) and (36) can be expressed in terms of mass operator. Let the mass operator $\overline{\overline{\hat{M}}}$ under QCA–CP be expressed as

$$\overline{\overline{\hat{M}}} = \sum_{s_j=1}^{L} n_{s_j} \int d\bar{r}_j \overline{\overline{\hat{C}}}_j^{s_j} \tag{37}$$

where

$$\overline{\overline{\hat{C}}}_l^{s_l} = \overline{\overline{\hat{t}}}_l^{s_l} + \sum_{s_j=1}^{L} n_{s_j} \int d\bar{r}_j h_{s_l s_j}(\bar{r}_j - \bar{r}_l) \overline{\overline{\hat{t}}}_l^{s_l} \overline{\overline{G}}_c \overline{\overline{\hat{C}}}_j^{s_j} \tag{38}$$

The average Green's operator under QCA–CP can be expressed as

$$E\left(\overline{\overline{G}}\right) = \overline{\overline{G}}_c = \overline{\overline{G}}_o + \overline{\overline{G}}_o \overline{\overline{\hat{M}}} \overline{\overline{G}}_c \tag{39}$$

In this case,

$$\left\langle \bar{p} \mid \overline{\overline{\widehat{M}}} \mid \bar{p}' \right\rangle = \langle \bar{p} \mid \bar{p}' \rangle \sum_{s_j=1}^{L} n_{s_j} \overline{\overline{\widehat{C}}}_p^{s_j} (\bar{p}, \bar{p}) \tag{40}$$

The mean Green's function then becomes

$$\overline{\overline{G}}(\bar{p}) = \left[\overline{\overline{G}}_o^{-1}(\bar{p}) - \overline{\overline{\widehat{M}}}(\bar{p}, \bar{p}) \right]^{-1} \tag{41}$$

and the dispersion relation is

$$\det \left[\overline{\overline{G}}_o^{-1}(\bar{p}) - \overline{\overline{\widehat{M}}}(\bar{p}, \bar{p}) \right] = 0 \tag{42}$$

Thus we can regard equations (26) and (37) as the mass operators under QCA and QCA–CP respectively.

3.3 Pair Distribution Functions for Media with Particles of Multiple Sizes

In applying QCA and QCA–CP to calculate the effective propagation constants, it is seen from (18), (19) and (35) that the results depend on the pair distribution functions for multi-species. The medium composed of N scatterers considered here is analogous to an ensemble of mixture of L types of particles in the study of statistical mechanics, by considering the dynamics and positions of the particles with regard to the interparticle forces. Studies have been made in obtaining the pair distribution functions using various approximate theories. One of the important results is based on the Percus–Yevick (PY) approximation.

The pair distribution function $g_{ij}(r)$ is proportional to the conditional probability of finding a particle of type j at a distance r from the origin given that there is a particle of type i at the origin. The total correlation function, $h_{ij}(r)$, is defined as

$$h_{ij}(r) = g_{ij}(r) - 1 \tag{43}$$

which describes the total influence of particle of species i on particle of species j. The direct correlation function, $c_{ij}(r)$, is related to $h_{ij}(r)$ by means of the generalized Ornstein–Zernike (OZ) relation [11,12]

$$h_{ij}(r) = c_{ij}(r) + \sum_{l=1}^{L} n_l \int d\bar{r}' c_{il}(r') h_{lj}(|\bar{r} - \bar{r}'|) \tag{44}$$

The physical interpretation of (44) is that the total correlation function can be decomposed into a sum of direct and indirect correlation functions, and the indirect influence of particle of species i on particle of species j is a result of particle of species i acting directly on a particle of species l at $\bar{r}'$, which in turn exerts total influence on particle of species j. The indirect influence is averaged over particle positions $\bar{r}'$ and particle species l and weighted by the number density n_l as indicated in (44).

In the following, we shall describe the results for non-interpenetrable spheres under the PY approximation. For non-interpenetrable spheres, the interparticle forces are zero except for the fact that two particles cannot interpenetrate each other. Let a_i and a_j be the particle radii of species i and j respectively. Then

$$g_{ij}(r) = 0 \qquad \text{for} \quad r < a_i + a_j \tag{45}$$

Under the PY approximation, it is assumed that for non-interpenetrable particles the direct correlation function $c_{ij}(r)$ is zero for separation larger than $a_i + a_j$. This physically means that any *net* interparticle influence between two particles for distance larger than $a_i + a_j$ is due to the presence of other particles and is attributed entirely to indirect influence. Thus,

$$c_{ij}(r) = 0 \qquad \text{for} \quad r > R_{ij} \tag{46}$$

where $R_{ij} = a_i + a_j$. Next, let

$$Y_{ij}(r) = \begin{cases} -c_{ij}(r) & \text{for} \quad r < R_{ij} \\ g_{ij}(r) & \text{for} \quad r \geq R_{ij} \end{cases} \tag{47}$$

Then using (43), (45)–(47), the OZ relation can be expressed entirely in terms of Y_{ij}

$$\begin{aligned} Y_{ij}(r) = 1 &+ \sum_{l=1}^{L} n_l \int_{r'<R_{lj};|\bar{r}-\bar{r}'|<R_{il}} d\bar{r}' Y_{il}(r') \\ &- \sum_{l=1}^{L} n_l \int_{r'<R_{lj};|\bar{r}-\bar{r}'|>R_{il}} d\bar{r}' \left[Y_{il}(\bar{r}-\bar{r}') - 1\right] Y_{lj}(r') \\ &\qquad\qquad i,j = 1,2,\ldots,L \end{aligned} \tag{48}$$

The solution of (48) for the case of single species has been solved by Wertheim, Thiele and Baxter. For the case of two species, the solution can be found in Lebowitz. For the case of general L species, the solution is obtained by Baxter based on a generalized Wiener–Hopf technique.

Let $\tilde{H}_{ij}(\bar{p})$ and $\tilde{C}_{ij}(\bar{p})$ be proportional to the three dimensional Fourier transform of $h_{ij}(\bar{r})$ and $c_{ij}(\bar{r})$ as follows

$$\tilde{H}_{ij}(\bar{p}) = (n_i n_j)^{1/2} \int d\bar{r} e^{i\bar{p}\cdot\bar{r}} h_{ij}(\bar{r}) \tag{49}$$

$$\tilde{C}_{ij}(\bar{p}) = (n_i n_j)^{1/2} \int d\bar{r} e^{i\bar{p}\cdot\bar{r}} c_{ij}(\bar{r}) \tag{50}$$

then in matrix form, the OZ relation becomes

$$\tilde{H}(p) = \tilde{C}(p) + \tilde{C}(p)\tilde{H}(p) \tag{51}$$

Because of the spherical particle assumption, the transform only depends on $p = |\bar{p}|$. In (51) all matrices are of dimensional $L \times L$. Based on the generalized Wiener–Hopf technique, the solution of the $L \times L$ matrix $\tilde{C}(p)$ can be factorized as [14]

$$\tilde{C}(p) = E - \tilde{Q}^T(-p)\tilde{Q}(p) \tag{52}$$

where E is the $L \times L$ unit matrix, and superscript T denotes transpose of the $L \times L$ matrix $\tilde{Q}$

$$\tilde{Q}_{ij}(p) = \delta_{ij} - \int_{S_{ij}}^{R_{ij}} dr e^{ipr} Q_{ij}(r) \tag{53}$$

δ_{ij} is the Kronecker delta, and

$$S_{ij} = a_i - a_j \tag{54}$$

$$R_{ij} = a_i + a_j \tag{55}$$

$$Q_{ij}(r) = 2\pi (n_i n_j)^{1/2} q_{ij}(r) \tag{56}$$

where $Q_{ij}(r)$ and $q_{ij}(r)$ are functions only nonzero over the range $S_{ij} \leq r \leq R_{ij}$. Note that S_{ij} can be negative. The solution of $q_{ij}(r)$

is [14]

$$q_{ij}(r) = A_i \frac{r^2}{2} + B_i r + D_{ij} \tag{57}$$

$$A_i = \frac{1 - \xi_3 + 6a_i\xi_2}{(1-\xi_3)^2} \tag{58}$$

$$B_i = -\frac{6a_i^2\xi_2}{(1-\xi_3)^2} \tag{59}$$

$$D_{ij} = -A_i\frac{R_{ij}^2}{2} - B_i R_{ij} \tag{60}$$

$$\xi_\alpha = \frac{\pi}{6}\sum_{j=1}^{L} n_j (2a_j)^\alpha \tag{61}$$

$$\alpha = 1, 2, 3.$$

The process of computation is as follows. By using (54)–(61), $Q_{ij}(r)$ for $S_{ij} \leq r \leq R_{ij}$ can be computed. Then, $Q_{ij}(p)$ is calculated by using (53). Next, the matrix $\tilde{C}(p)$ is evaluated by using (52).

Next the matrix equation of (51) is solved and $\tilde{H}(p)$ is calculated. Then, $h_{ij}(r) = g_{ij}(r) - 1$ is computed by taking an inverse Fourier transform. In this manner, the pair distribution function $g_{ij}(r)$ is calculated and is numerically illustrated in Figs. 3.3.1–3.3.6.

In the QCA and QCA–CP equations $H_{s_i s_j}(p)$ as defined by (19) is needed. Comparing (19) and (49) gives

$$H_{ij}(\bar{p}) = \frac{\tilde{H}_{ij}(-\bar{p})}{(2\pi)^3 (n_i n_j)^{1/2}} \tag{62}$$

In Fig. 3.3.1, the pair distribution functions for the case of particles of identical sizes are plotted for $f = 0.2$ and $f = 0.4$. We see that the conditional probability is zero for the separation less than one diameter of particle because the particles cannot interpenetrate each other. For higher concentration of particles, the pair distribution function shows more variations indicating that the particles have less freedom in positioning themselves.

In Fig. 3.3.2, the pair distribution functions for a mixture of two particle sizes are plotted with $a_2 = 2a_1$, $f_1 = 0.03$, and $f_2 = 0.01$. Because of small fractional volumes in this case, the pair distribution functions show only a small deviation from the results of hole correction

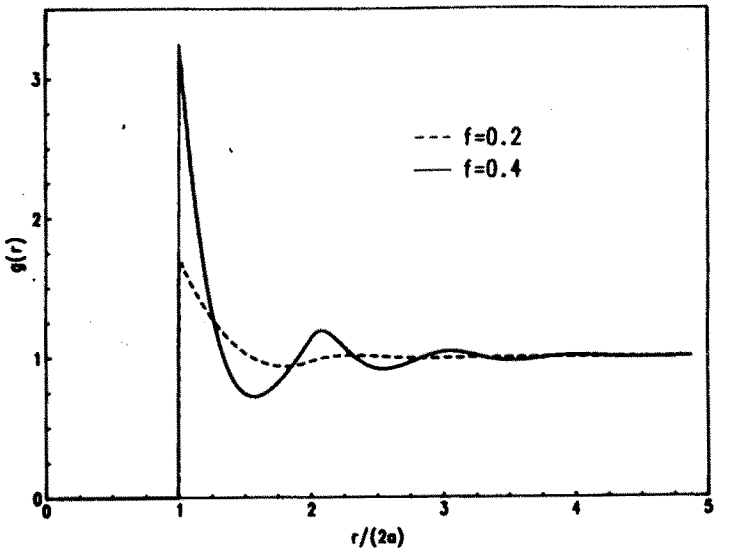

Figure 3.3.1 Percus–Yevick results of $g(r)$, for $f = 0.2$, and $f = 0.4$, vs $r/(2a)$.

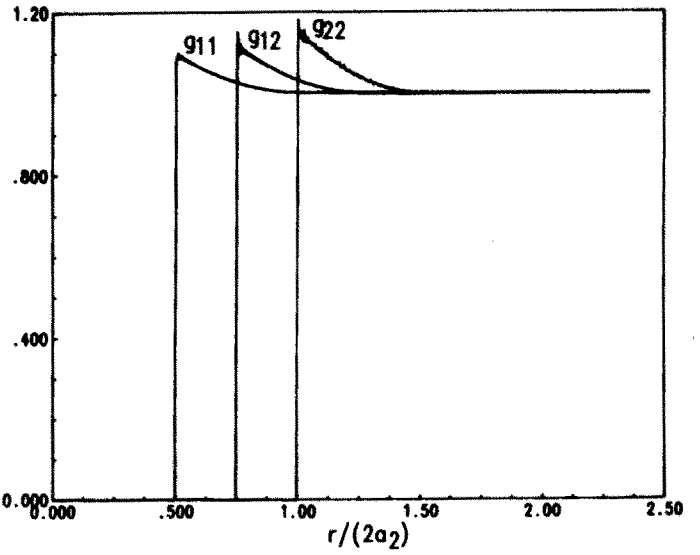

Figure 3.3.2 Percus–Yevick results of $g_{ij}(r)$, $i, j = 1, 2$, for $f_1 = 0.03$, and $f_2 = 0.01$, vs $r/(2a_2)$, $a_2 = 2a_1$.

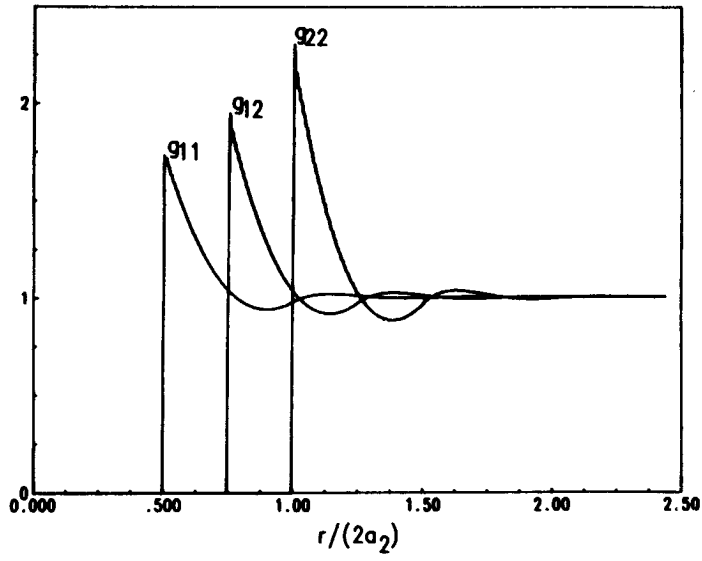

Figure 3.3.3 Percus–Yevick results of $g_{ij}(r)$, $i, j = 1, 2$, for $f_1 = 0.2$, and $f_2 = 0.01$, vs $r/(2a_2)$, $a_2 = 2a_1$.

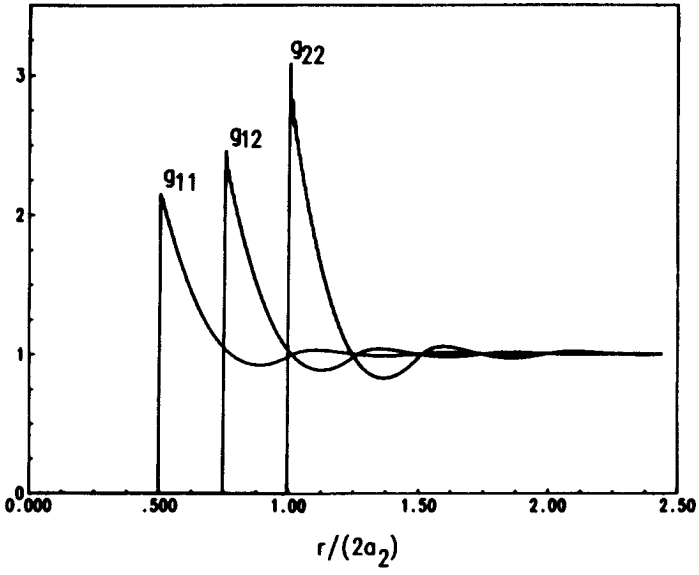

Figure 3.3.4 Percus–Yevick results of $g_{ij}(r)$, $i, j = 1, 2$, for $f_1 = 0.2$, and $f_2 = 0.1$, vs $r/(2a_2)$, $a_2 = 2a_1$.

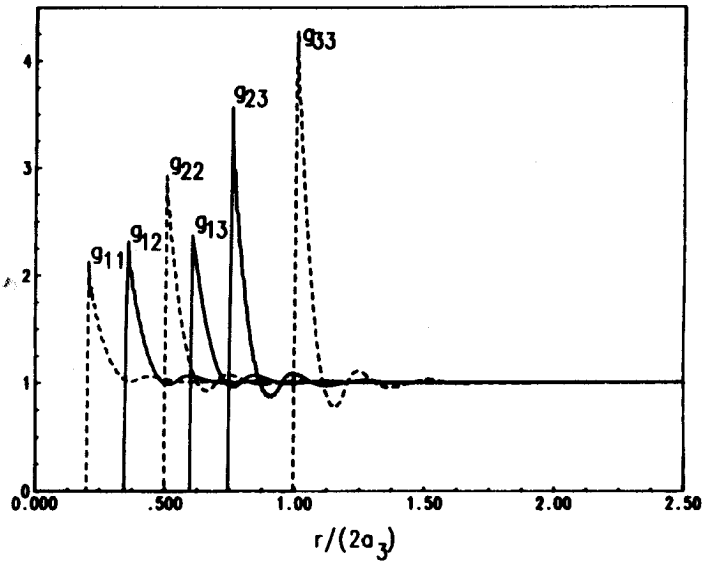

Figure 3.3.5 Percus–Yevick results of $g_{ij}(r)$, $i, j = 1, 2, 3$, for $f_1 = 0.15$, $f_2 = 0.1$, and $f_3 = 0.05$, vs $r/(2a_3)$, $a_3 = 5a_1$, $a_2 = 2.5a_1$.

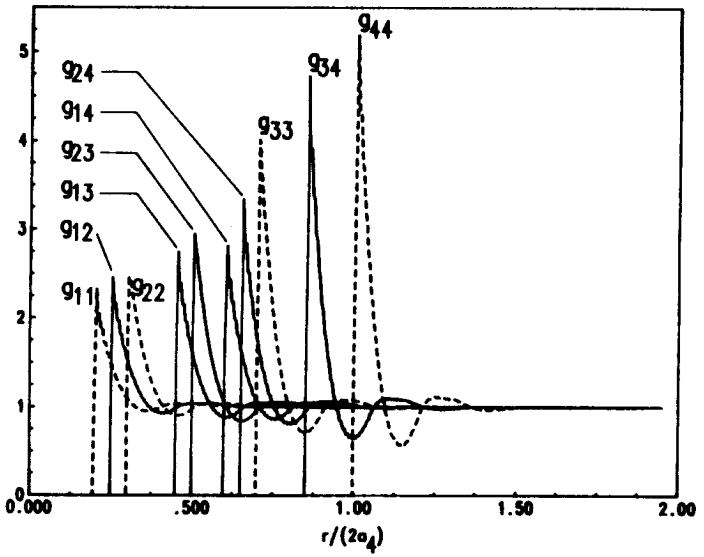

Figure 3.3.6 Percus–Yevick results of $g_{ij}(r)$, $i, j = 1, 2, 3, 4$, for $f_1 = 0.15$, $f_2 = 0.1$, $f_3 = 0.05$, and $f_4 = 0.02$, vs $r/(2a_4)$, $a_4 = 5a_1$, $a_3 = 3.5a_1$, $a_2 = 1.5a_1$.

(HC). In the HC approximation,

$$g_{ij}(r) = \begin{cases} 0 & r < a_i + a_j \\ 1 & r \geq a_i + a_j \end{cases} \tag{63}$$

When the pair distribution function is equal to 1, the two particle positions are independent. Thus, the hole correction approximation assumes that the particles are independent aside from the fact that they cannot interpenetrate each other. The deviation of pair distribution function from unity is a measure of the *freedom* of particle positions with larger deviation corresponding to a smaller freedom.

In Figs. 3.3.3 and 3.3.4, particle concentrations are higher so that the deviations of pair functions from unity are significant with less freedom for larger concentrations. The results also indicate that g_{22} is more different from unity than g_{11}. This is true in spite of the fact that the fractional volume of particle size 2 in both figures are small because the high concentration of particle size 1 affects the freedom of positions of particle size 2. Also, g_{22} is more different from unity because particles have less freedom in positions as particle size 2 becomes larger and larger. Fractional volume of particle size 2 in Fig. 3.3.4 is higher than that in Fig. 3.3.3 while fractional volume of particle size 1 is the same in both figures. Nevertheless, the increase in concentrations of particle size 2 affects that of particle size 1 as indicated in the figures. In Fig. 3.3.5, the results of a mixture of particles with three different sizes are illustrated with $a_3 > a_2 > a_1$. We see that g_{33} exhibit the least freedom while there is more freedom in g_{11} than in g_{22}. We also note that the value of g_{ij} generally lies between g_{ii} and g_{jj}. In Fig. 3.3.6, the results of the pair distribution functions for a medium containing particles of four different sizes are also illustrated. Because of the symmetry relation $g_{ij} = g_{ji}$, there are 10 pair distribution functions for this case as illustrated in the figure.

3.4 Effective Propagation Constants for Media with Small Particles

To calculate the effective propagation constants for QCA and QCA–CP, we need to solve the integral equations (18) and (35). In general, it requires numerical techniques to solve the integral equations for cases where particle sizes are comparable to or larger than wavelengths.

The numerical technique for calculating the effective propagation constant for moderate size particles under QCA will be discussed in section 3.5. In this section, we consider the case of small particles. Closed form expressions of the effective propagation constants can be derived in the low-frequency limit when particles are much smaller than wavelength. The results facilitate the understanding of effective attenuation rates and effective phase velocity for wave propagation in discrete random medium of multiple species.

The effective propagation constant is denoted by $K = K_r + iK_i$. The real part K_r is related to the effective phase velocity while he imaginary part K_i is related to the attenuation. Generally, $K_r \gg K_i$. We shall, in solving (18) and (35), (i) keep only the leading term of the real part and the leading term of the imaginary part and (ii) ignore terms of order less than $(ka)^3$ [2,8].

a. QCA

The momentum representation of $\overline{\overline{T}}^{s_j}$, $\overline{\overline{T}}_p^{s_j}(\bar{p},\bar{p}')$, can be calculated by using the mixed representation [2,8]. In the low-frequency limit

$$\overline{\overline{T}}_p^{s_j}(\bar{p},\bar{p}') = T_m^{s_j} v_{s_j} \overline{\overline{I}} \tag{64}$$

where $v_{s_j} = (4\pi/3)a_{s_j}^3$ is the volume of s_j type particle, and

$$T_m^{s_j} = 3k^2 y_{s_j}\left[1 + i\frac{2}{3}k^3 a_{s_j}^3 y_{s_j}\right] \tag{65}$$

$$y_{s_j} = \frac{\epsilon_{s_j} - \epsilon}{\epsilon_{s_j} + 2\epsilon} \tag{66}$$

Further, let $\overline{\overline{C}}_p^{s_j}(\bar{p},\bar{p}') = C_{s_j}\overline{\overline{I}}$ in the low-frequency limit. Using (64) in (18) gives the relation

$$C_{s_j} = T_m^{s_j} v_{s_j} + T_m^{s_j} v_{s_j} \sum_{s_l=1}^{L} n_{s_l} C_{s_l}\left[\frac{1}{3k^2} + i\frac{4\pi^2 k}{3} H_{s_j s_l}(\bar{p}=0)\right] \tag{67}$$

By keeping only the leading term in the real part and the leading term in the imaginary part, equation (67) can be solved for C_{s_j}. Substituting $\overline{\overline{C}}_p^{s_j}(\bar{p},\bar{p})$ into the dispersion relation (22), the effective propagation K^2 can be solved and is given by

$$K^2 = k^2 + \sum_{s_j=1}^{L} n_{s_j} C_{s_j} \tag{68}$$

After simplification, this gives

$$K^2 = k^2 + \frac{3k^2}{D} \sum_{s_j=1}^{L} f_{s_l} y_{s_l} \times \left\{ 1 + i\frac{2k^3}{3D} \left[a_{s_l}^3 y_{s_l} + \sum_{s_j=1}^{L} a_{s_j}^3 8\pi^3 n_{s_j} y_{s_j} H_{s_j s_l}(\bar{p}=0) \right] \right\} \quad (69)$$

where

$$D = 1 - \sum_{s_l=1}^{L} f_{s_l} y_{s_l} \quad (70)$$

and

$$f_{s_j} = n_{s_j} \frac{4\pi}{3} a_{s_j}^3 \quad (71)$$

is the fractional volume occupied by particles of type s_j.

b. QCA-CP

The low frequency QCA–CP solution can be obtained by solving (33), (35) and (36). The solution for (33) is

$$\hat{\bar{\bar{t}}}_p^{s_j}(\bar{p},\bar{p}') = \hat{t}_m^{s_j} v_{s_j} \bar{\bar{I}} \quad (72)$$

where

$$\hat{t}_m^{s_j} = 3K^2 \hat{y}_{s_j} \left[1 + i\frac{2}{3} K^3 a_{s_j}^3 \hat{y}_{s_j} \right] \quad (73)$$

$$\hat{y}_{s_j} = \frac{k_{s_j}^2 - k^2}{3K^2 + \left(k_{s_j}^2 - k^2\right)} \quad (74)$$

Solving (35) and (36) gives a nonlinear equation for the effective propagation constant as follows

$$\hat{\bar{\bar{C}}}_p^{s_j}(\bar{p},\bar{p}') = \hat{C}_{s_j} \bar{\bar{I}} \quad (75)$$

$$\hat{C}_{s_j} = \hat{t}_m^{s_j} v_{s_j} + \hat{t}_m^{s_j} v_{s_j} \sum_{s_l=1}^{L} n_{s_l} \hat{C}_{s_l} \left[\frac{1}{3K^2} + i\frac{4\pi^2 K}{3} H_{s_j s_l}(\bar{p}=0) \right] \quad (76)$$

$$K^2 = k^2 + \sum_{s_j=1}^{L} n_{s_j} \widehat{C}_{s_j}$$

$$= k^2 + \frac{3K^2}{\widehat{D}} \sum_{s_l=1}^{L} f_{s_l} \widehat{y}_{s_l}$$

$$\times \left\{ 1 + i\frac{2K^3}{3\widehat{D}} \left[a_{s_l}^3 \widehat{y}_{s_l} + \sum_{s_j=1}^{L} a_{s_j}^3 8\pi^3 n_{s_j} \widehat{y}_{s_j} H_{s_j s_l}(\overline{p}=0) \right] \right\} \quad (77)$$

$$\widehat{D} = 1 - \sum_{s_l=1}^{L} f_{s_l} \widehat{y}_{s_l} \quad (78)$$

Note that $\widehat{y}_{s_j}$ depends on K^2 so that (77) is a nonlinear equation of K^2. Solution of (77) for K^2 can be conveniently computed in the following manner. First, the terms in the square bracket in (77) are ignored. The remaining terms can be cast into a polynomial equation for K^2 which can be solved readily. Experience indicates that only one solution of K^2 has the correct physical meaning of effective propagation constant. This solution is used as an initial approximation and inserted into the right hand side of (77). The solution quickly converges after a few iterations.

Thus solutions (69) and (77) give K^2 under QCA and QCA–CP respectively. The real part of K is the angular frequency divided by the effective phase velocity. The imaginary part of K gives effective attenuation rate due to both absorption and scattering.

In Figs. 3.4.1 to 3.4.10, by solving the equations (69) and (77), we illustrate the normalized attenuation rate $2K_i/k$ and the effective dielectric constant $(K^2/k^2)_r$ where subscripts r and i denote real and imaginary parts respectively. The parameters chosen represent typical values found in microwave and millimeter wave remote sensing in snow. Dry snow is a mixture of ice particles and air with fractional volume of ice between 0.2 and 0.4. The permittivity of ice particles is $3.2\epsilon_o$. The ice particles are not of identical sizes and are usually described by a particle size distribution ranging from 0.01 mm to 2 mm. Wet snow is a mixture of air, ice particles and water droplet with sizes of water droplets comparable to that of ice particles [27,28].

In Figs. 3.4.1 and 3.4.2, the case of particles of identical sizes is considered. The attenuation rate $2K_i/k$ and the effective dielectric constant $(K^2/k^2)_r$ are plotted as a function of f for $ka = 0.1047$

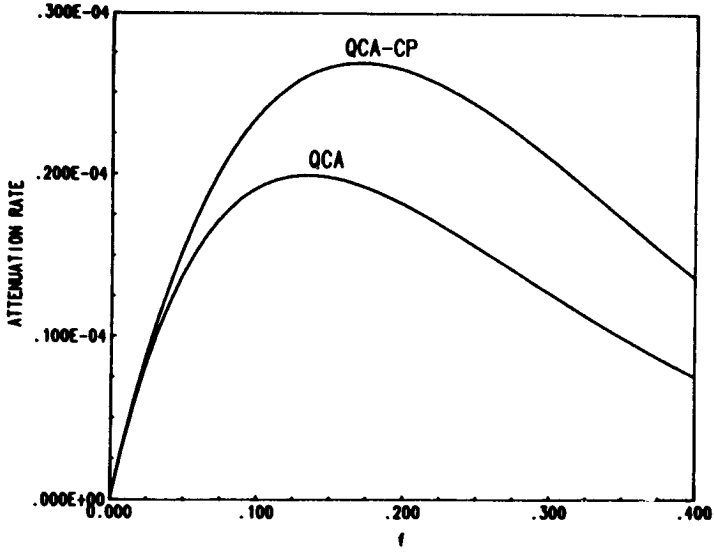

Figure 3.4.1 Attenuation rate $2K_i/k$ as a function of f, for $ka = 0.1047$, and $\epsilon = 3.2\epsilon$, $\epsilon = \epsilon_o$ is the background permittivity. The results of Quasicrystalline Approximation (QCA) and Quasicrystalline Approximation with Coherent Potential (QCA–CP) are compared.

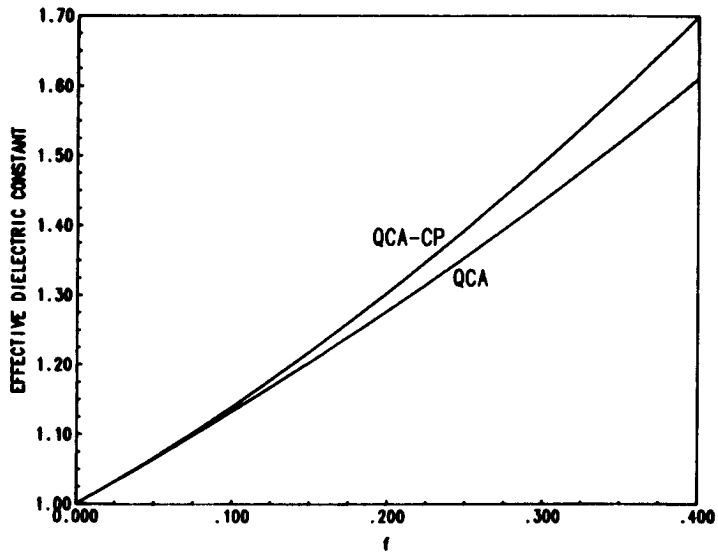

Figure 3.4.2 Effective dielectric constant $(K^2/k^2)_r$ as a function of f, for $ka = 0.1047$, and $\epsilon = 3.2\epsilon$, $\epsilon = \epsilon_o$ is the background permittivity. The results of QCA and QCA–CP are compared.

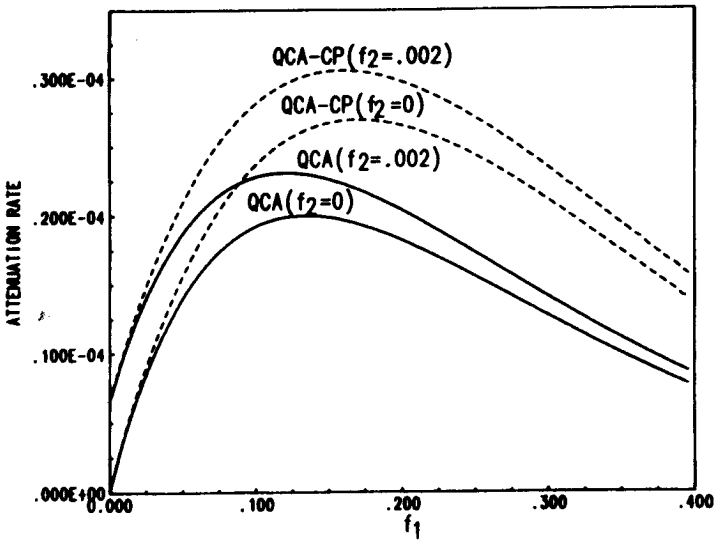

Figure 3.4.3 Attenuation rate $2K_i/k$ as a function of f_1, for (1) $f_2 = 0$ and (2) $f_2 = 0.002$, where $ka_1 = 0.1047$, $ka_2 = 0.2094$, and $\epsilon_1 = \epsilon_2 = 3.2\epsilon$, $\epsilon = \epsilon_o$ is the background permittivity. The results of Quasicrystalline Approximation (QCA) and Quasicrystalline Approximation with Coherent Potential (QCA–CP) are compared.

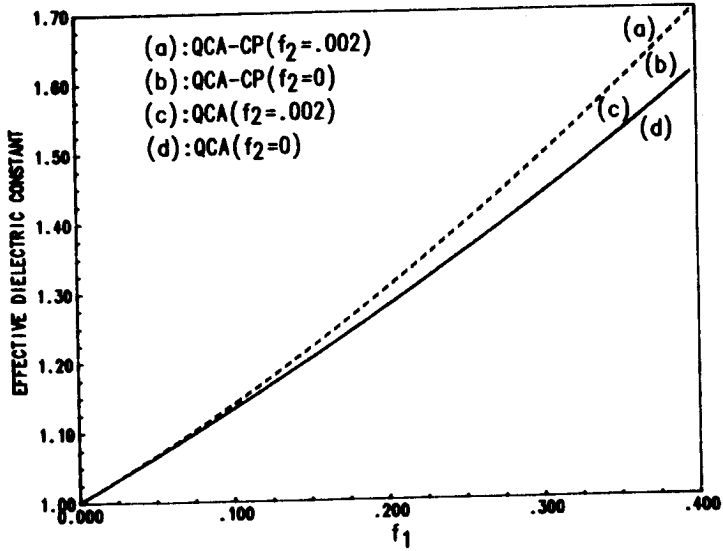

Figure 3.4.4 Effective dielectric constant $(K^2/k^2)_r$ as a function of f_1, for (1) $f_2 = 0$ and (2) $f_2 = 0.002$, where $ka_1 = 0.1047$, $ka_2 = 0.2094$, and $\epsilon_1 = \epsilon_2 = 3.2\epsilon$, $\epsilon = \epsilon_o$ is the background permittivity. The results of QCA and QCA–CP are compared.

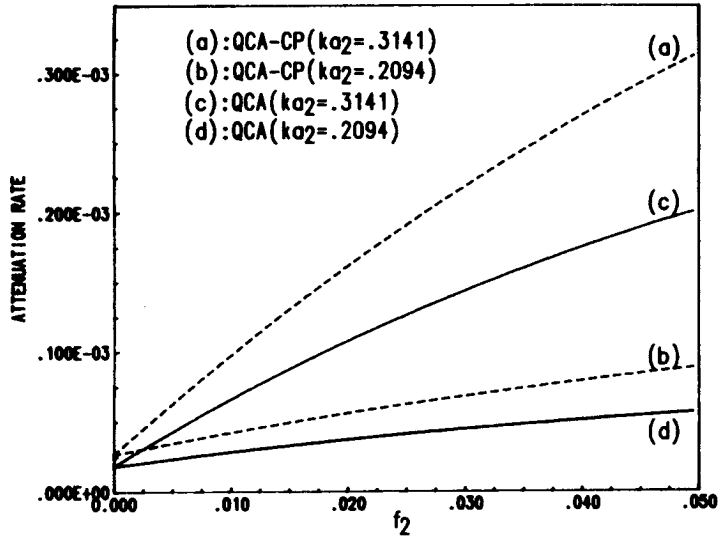

Figure 3.4.5 Attenuation rate $2K_i/k$ as a function of f_2, for (1) $ka_2 = 0.2094$ and (2) $ka_2 = 0.3141$, where $f_1 = 0.2$, $ka_1 = 0.1047$, $\epsilon_1 = \epsilon_2 = 3.2\epsilon$, $\epsilon = \epsilon_o$ is the background permittivity.

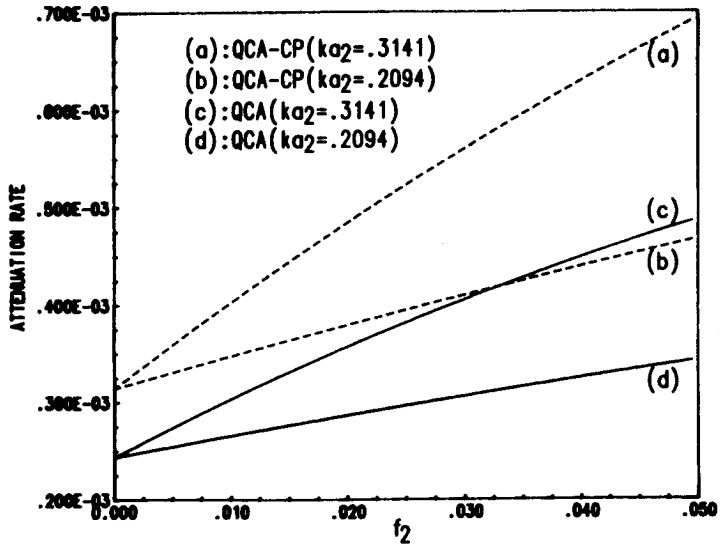

Figure 3.4.6 Attenuation rate $2K_i/k$ as a function of f_2, for (1) $ka_2 = 0.2094$ and (2) $ka_2 = 0.3141$, where $f_1 = 0.2$, $ka_1 = 0.1047$, $\epsilon_1 = \epsilon_2 = 3.2(1 + i0.001)\epsilon$, $\epsilon = \epsilon_o$ is the background permittivity.

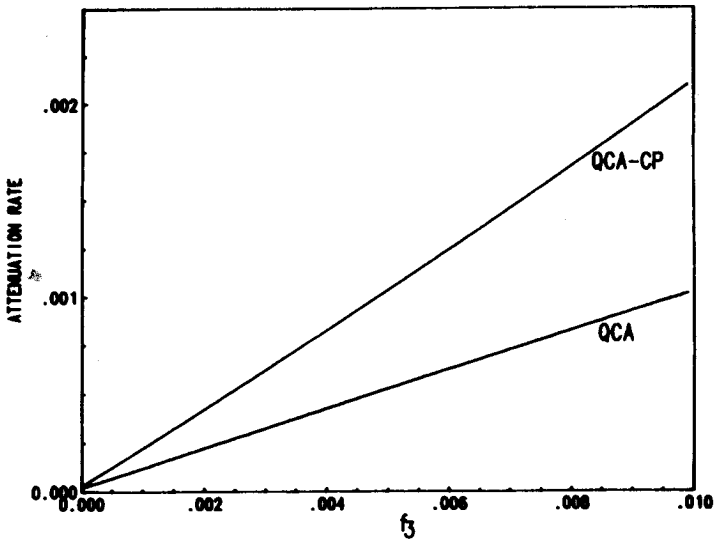

Figure 3.4.7 Attenuation rate $2K_i/k$ as a function of f_3, for $f_1 = 0.2$, and $f_2 = 0.002$, where $ka_1 = 0.1047$, $ka_2 = 0.2094$, $ka_3 = 0.3141$, and $\epsilon_1 = \epsilon_2 = 3.2\epsilon$, $\epsilon_3 = 66.2(1 + i0.55)\epsilon$, $\epsilon = \epsilon_o$ is the background permittivity.

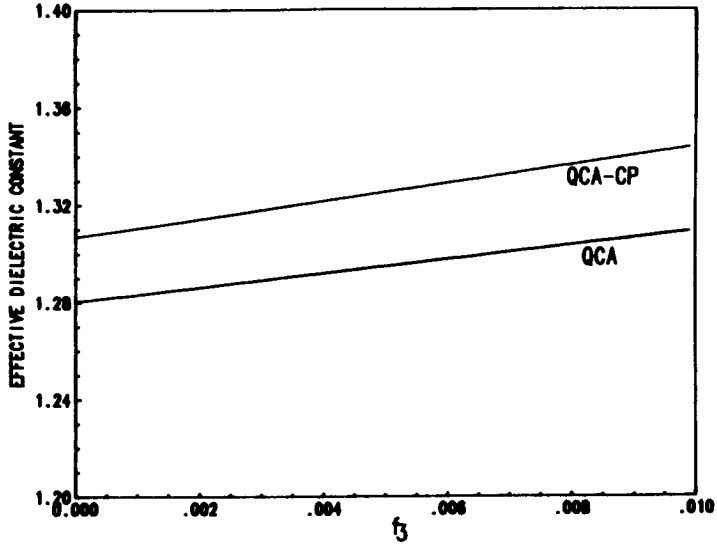

Figure 3.4.8 Effective dielectric constant $(K^2/k^2)_r$ as a function of f_3, for $f_1 = 0.2$, and $f_2 = 0.002$, where $ka_1 = 0.1047$, $ka_2 = 0.2094$, $ka_3 = 0.3141$, and $\epsilon_1 = \epsilon_2 = 3.2\epsilon$, $\epsilon_3 = 66.2(1 + i0.55)\epsilon$, $\epsilon = \epsilon_o$ is the background permittivity.

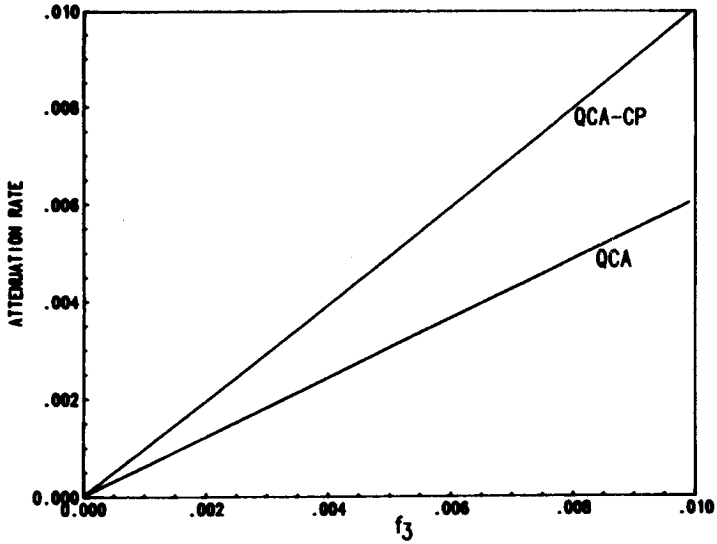

Figure 3.4.9 Attenuation rate $2K_i/k$ as a function of f_3, for $f_1 = 0.2$, and $f_2 = 0.002$, where $ka_1 = 0.1047$, $ka_2 = 0.2094$, $ka_3 = 0.3141$, and $\epsilon_1 = \epsilon_2 = 3.2\epsilon$, $\epsilon_3 = 6.205(1 + i1.224)\epsilon$, $\epsilon = \epsilon_o$ is the background permittivity.

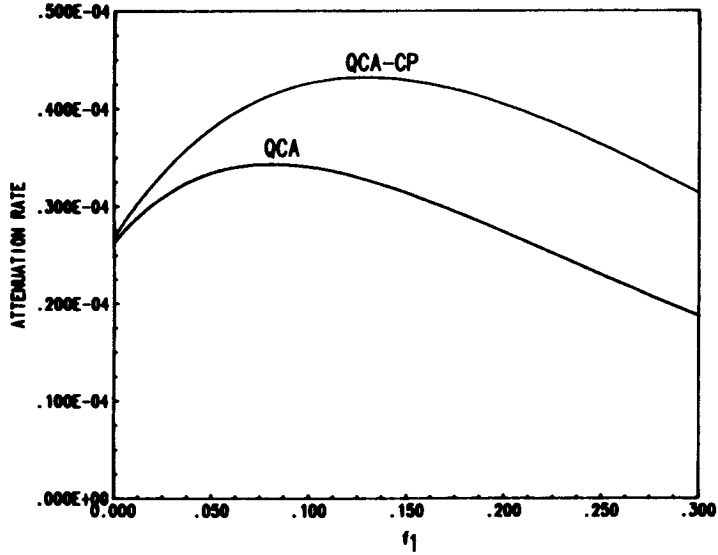

Figure 3.4.10 Attenuation rate $2K_i/k$ as a function of f_1, for $f_2 = 0.005$, $f_3 = 0.003$, and $f_4 = 0.001$, where $ka_1 = 0.1047$, $ka_2 = 0.1571$, $ka_3 = 0.2094$, $ka_4 = 0.3141$, and $\epsilon_1 = \epsilon_2 = \epsilon_3 = \epsilon_4 = 3.2\epsilon$, $\epsilon = \epsilon_o$ is the background permittivity.

and for real particle permittivity $\epsilon_s = 3.2\epsilon_o$. In this case there is no absorption. Attenuation is due entirely to scattering. We note that the attenuation rate first increase with f, then rises to a peak and decreases when f further increases. This indicates that the medium appears more homogeneous as the particle concentration further increases beyond a certain value.

In Figs. 3.4.3 and 3.4.4, the attenuation rate $2K_i/k$ and the effective dielectric constant $(K^2/k^2)_r$ are illustrated respectively as a function of f_1 for $f_2 = 0$ and $f_2 = 0.002$. The two particle sizes are $ka_1 = 0.1047$ and $ka_2 = 0.2094$. The results based on QCA and QCA–CP are illustrated. In spite of the much smaller fractional volume $(f_2 = 0.002)$, larger particles have a larger weighting factor in scattering and can contribute significantly to the scattering attenuation rates. This indicates that it is generally not valid to use the average particle size to calculate the scattering effects. On the other hand, Fig. 3.4.4 shows that the larger particles with a very small fractional volume have relatively a small effect on the effective dielectric constant. The results in Fig. 3.4.3 also indicate that QCA–CP generally predicts a larger scattering attenuation rate than QCA. This is apparent by comparing equations (6) and (33). The scattering operator for a single scatterer for QCA is embedded in medium with propagator $\overline{\overline{G}}_o$. For QCA–CP, the single particle transition operator $\overline{\overline{t}}_j$ is embedded in an effective medium with propagator $\overline{\overline{G}}_c$.

In Fig. 3.4.5, the attenuation rates are plotted as a function of f_2 with $f_1 = 0.2$. Because the concentration of f_2 is small, the attenuation rate increases almost linearly with f_2. In Fig. 3.4.6, the attenuation rates are illustrated for the case of slightly lossy particles with $\epsilon_1 = \epsilon_2 = 3.2(1+i0.001)\epsilon_o$. The particle sizes in the figure are such that the attenuation rate due to absorption is comparable to that due to scattering. In Figs. 3.4.7–3.4.9, we illustrate the case when the medium is a mixture of three particle species with different sizes and permittivities. In Figs. 3.4.7 and 3.4.8, particles of species 3 are largest in size and have permittivity equal to $\epsilon_3 = 66.2(1+i0.55)\epsilon_o$ corresponding to that of water at 5 GHz. In Fig. 3.4.9, $\epsilon_3 = 6.205(1+i1.224)\epsilon_o$ which corresponds to that of water at 90 GHz. Thus the model can be used to represent wet snow. We note that both the effective dielectric constant and the attenuation rate increases rapidly with f_3 which corresponds to wetness content of wet snow. In Fig. 3.4.10, we illustrate the case when there are four different particle sizes.

c. Dielectric Mixing Formula Ignoring Scattering Attenuation Rates

Classical dielectric mixing formulae aim at calculating the effective permittivity of a mixture of components. For these cases, the particle size is much smaller than wavelength so that scattering attenuation rates can be ignored. Such dielectric mixing formula can be obtained from the results of effective propagation constants by setting particle size a_{s_j} to zero and number density n_{s_j} to infinity such that fractional volume f_{s_j} of (71) remains finite. The effective permittivity ϵ_{eff} is given by

$$\frac{\epsilon_{eff}}{\epsilon} = \frac{K^2}{k^2} \tag{79}$$

d. Mixing Formula for QCA

From (69), we get the mixing formula

$$\frac{\epsilon_{eff}}{\epsilon} = 1 + \frac{3\sum_{s_j=1}^{L} f_{s_j} y_{s_j}}{1 - \sum_{s_j=1}^{L} f_{s_j} y_{s_j}} \tag{80}$$

Using expression for y_{s_j} as given by (66), the QCA result of (80) can be rearranged to give

$$\frac{\epsilon_{eff} - \epsilon}{\epsilon_{eff} + 2\epsilon} = \sum_{s_j=1}^{L} f_{s_j} \frac{\epsilon_{s_j} - \epsilon}{\epsilon_{s_j} + 2\epsilon} \tag{81}$$

which is the same as the classical Rayleigh mixing formula [29].

e. Mixing Formula for QCA-CP

The mixing formula for QCA-CP, from (77) and (74), is

$$\epsilon_{eff} = \epsilon + \frac{3\epsilon_{eff} \sum_{s_j=1}^{L} f_{s_j} \frac{\epsilon_{s_j} - \epsilon}{3\epsilon_{eff} + \epsilon_{s_j} - \epsilon}}{1 - \sum_{s_j=1}^{L} f_{s_j} \frac{\epsilon_{s_j} - \epsilon}{3\epsilon_{eff} + \epsilon_{s_j} - \epsilon}} \tag{82}$$

3.5 Effective Propagation Constants for Media with Moderate Size Particles

Generally, for cases where particle sizes are comparable to or larger than wavelengths, it requires numerical technique to solve for the effective propagation constants. Such cases will be illustrated using the quasicrystalline approximation. We also find it convenient to use the T-matrix formulism with vector spherical wave functions as basis to formulate the multiple scattering equation and dispersion relation [4,8].

Let $\overline{E}^{inc}(\overline{r})$ be the incident electric field in a medium with multispecies of particles and $\overline{E}_j^S(\overline{r})$ be the scattered field form the j th particle. The total field $\overline{E}(\overline{r})$ at point $\overline{r}$ is the sum of the incident field and the scattered fields from all particles,

$$\overline{E}(\overline{r}) = \overline{E}^{inc}(\overline{r}) + \sum_{j=1}^{N} \overline{E}_j^S(\overline{r}) \tag{83}$$

The scattered field $\overline{E}_j^S(\overline{r})$ is related to the j th particle exciting field $\overline{E}_j^E(\overline{r})$ by

$$\overline{E}_j^S(\overline{r}) = \overline{\overline{T}}_j^{s_j} \overline{E}_j^E(\overline{r}) \tag{84}$$

where $\overline{\overline{T}}_j^{s_j}$ is the transition operator for the particle j of the s_j species. The exciting field for the j th particle can also be expressed as the total field less its own scattered field

$$\begin{aligned}\overline{E}_j^E(\overline{r}) &= \overline{E}^{inc}(\overline{r}) + \sum_{l\neq j}^{N} \overline{E}_l^S(\overline{r}) \\ &= \overline{E}^{inc}(\overline{r}) + \sum_{l\neq j}^{N} \overline{\overline{T}}_l^{s_l} \overline{E}_l^E(\overline{r})\end{aligned} \tag{85}$$

with $j = 1, \ldots, N$.

Under the quasicrystalline approximation, the integral equation for the conditional average of the j th particle exciting field, $\left\langle \overline{E}_j^E(\overline{r}) \right\rangle_j$, is

$$\left\langle \overline{E}_j^E(\overline{r}) \right\rangle_j = \overline{E}^{inc}(\overline{r}) + \sum_{s_l=1}^{L} n_{s_l} \int d\overline{r}_l \, g_{s_j s_l}(\overline{r}_l, \overline{r}_j) \overline{\overline{T}}_l^{s_l} \left\langle \overline{E}_l^E(\overline{r}) \right\rangle_l \tag{86}$$

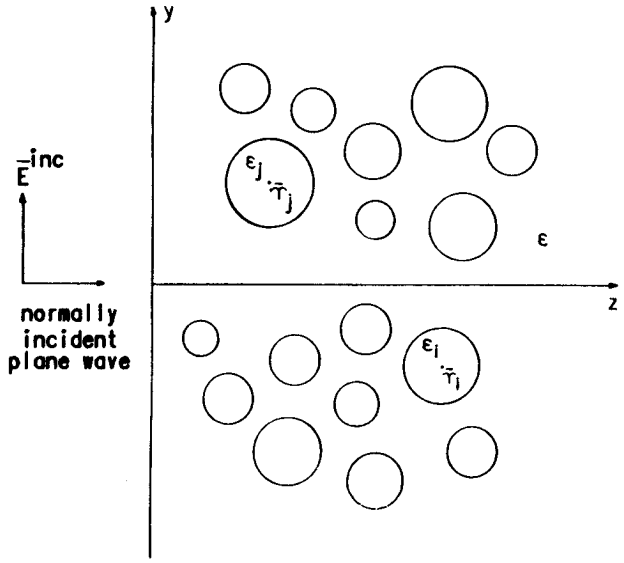

Figure 3.5.1 Plane electromagnetic wave normally incident on a half space of multiple species of particles with different sizes and permittivities.

where $\overline{\overline{T}}_l^{s_l} \left\langle \overline{E}_l^E(\bar{r}) \right\rangle_l$ is the field scattered by a scatterer of s_l species at $\bar{r}_l$ when excited by the field $\left\langle \overline{E}_l^E(\bar{r}) \right\rangle_l$.

For a plane electromagnetic wave normally incident on a half-space of spherical scatterers (Fig. 3.5.1), the incident field is $\overline{E}^{inc}(\bar{r}) = \hat{y}e^{ikz}$ and can be expanded in vector spherical waves

$$\overline{E}_{inc}(\bar{r}) = e^{ikz_j} \sum_{n=1}^{\infty} \frac{i^n}{2} \sqrt{4\pi(2n+1)} \left[Rg\overline{M}_{1n}(k\overline{rr_j}) - Rg\overline{M}_{-1n}(k\overline{rr_j}) + Rg\overline{N}_{1n}(k\overline{rr_j}) + Rg\overline{N}_{-1n}(k\overline{rr_j}) \right] \tag{87}$$

where $Rg\overline{M}_{mn}(k\overline{rr_j})$ and $Rg\overline{N}_{mn}(k\overline{rr_j})$ are regular vector spherical wave functions [8,30]

$$Rg\overline{M}_{mn}(k\bar{r}) = \sqrt{\frac{(2n+1)(n-m)!}{4\pi n(n+1)(n+m)!}} \overline{\nabla} \times \left[\bar{r} j_n(kr) P_n^m(\cos\theta) e^{im\phi} \right] \tag{88}$$

$$Rg\overline{N}_{mn}(k\bar{r}) = \frac{1}{k} \overline{\nabla} \times Rg\overline{M}_{mn}(k\bar{r}) \tag{89}$$

and $j_n(kr)$ is the spherical Bessel function and $P_n^m(\cos\theta)$ is the associated Legendre polynomial. The symbol $\overline{rr_j}$ is used to denote the vector pointing from $\overline{r}_j$ to $\overline{r}$. To solve (86), we express the exciting field and the scattered field in terms of vector spherical waves. At a point $\overline{r}$ in the vicinity of the j th particle, let [4,8]

$$\left\langle \overline{E}_j^E(\overline{r}) \right\rangle_j = \sum_{\nu=1}^{\infty} \sum_{\mu=-\nu}^{\nu} \left[a_{\mu\nu}^{sj}(z_j) Rg\overline{M}_{\mu\nu}(k\overline{rr_j}) + b_{\mu\nu}^{sj}(z_j) Rg\overline{N}_{\mu\nu}(k\overline{rr_j}) \right] \tag{90}$$

Then, for scattering by spheres

$$\overline{\overline{T}}_l^{s_l} \left\langle \overline{E}_l^E(\overline{r}) \right\rangle_l = \sum_{n=1}^{\infty} \sum_{m=-n}^{n} \left[T_n^{(M)s_l} a_{mn}^{s_l}(z_l) \overline{M}_{mn}(k\overline{rr_l}) + T_n^{(N)s_l} b_{mn}^{s_l}(z_l) \overline{N}_{mn}(k\overline{rr_l}) \right] \tag{91}$$

where $\overline{M}_{mn}(k\overline{rr_j})$ and $\overline{N}_{mn}(k\overline{rr_j})$ are vector spherical functions with the spherical Bessel function j_n in (88) and (89) replaced by spherical Hankel function of the first kind h_n, and $a_{\mu\nu}^{sj}, b_{\mu\nu}^{sj}, a_{mn}^{s_l}, b_{mn}^{s_l}$ are the unknown expansion coefficients. The scattering coefficients, $T_n^{(M)s_l}$ and $T_n^{(N)s_l}$ for spheres with radius a_{s_l} and permittivity ϵ_{s_l}, are those of Mie scattering [4,8]

$$T_n^{(M)s_l} = -\frac{[\rho_{s_l} j_n(\rho_{s_l})]' j_n(\zeta_{s_l}) - [\zeta_{s_l} j_n(\zeta_{s_l})]' j_n(\rho_{s_l})}{[\rho_{s_l} h_n(\rho_{s_l})]' j_n(\zeta_{s_l}) - [\zeta_{s_l} j_n(\zeta_{s_l})]' h_n(\rho_{s_l})} \tag{92}$$

$$T_n^{(N)s_l} = -\frac{[\rho_{s_l} j_n(\rho_{s_l})]' \zeta_{s_l}^2 j_n(\zeta_{s_l}) - [\zeta_{s_l} j_n(\zeta_{s_l})]' \rho_{s_l}^2 j_n(\rho_{s_l})}{[\rho_{s_l} h_n(\rho_{s_l})]' \zeta_{s_l}^2 j_n(\zeta_{s_l}) - [\zeta_{s_l} j_n(\zeta_{s_l})]' \rho_{s_l}^2 h_n(\rho_{s_l})} \tag{93}$$

where $\rho_{s_l} = ka_{s_l}$ and $\zeta_{s_l} = k_{s_l} a_{s_l}$. We can further make use of the vector translational addition theorem to expand the spherical vector waves $\overline{M}_{mn}(k\overline{rr_l})$ and $\overline{N}_{mn}(k\overline{rr_l})$ about $\overline{r}_j$ as center. Since $|\overline{r} - \overline{r}_j| < |\overline{r}_j - \overline{r}_l|$, the vector translational addition theorem is [8,30–33]

$$\overline{M}_{mn}(k\overline{rr_l}) = \sum_{\nu=1}^{\infty} \sum_{\mu=-\nu}^{\nu} \left[A_{\mu\nu mn}(k\overline{r_j r_l}) Rg\overline{M}_{\mu\nu}(k\overline{rr_j}) + B_{\mu\nu mn}(k\overline{r_j r_l}) Rg\overline{N}_{\mu\nu}(k\overline{rr_j}) \right] \tag{94}$$

$$\overline{N}_{mn}(k\overline{rr_l}) = \sum_{\nu=1}^{\infty} \sum_{\mu=-\nu}^{\nu} \left[B_{\mu\nu mn}(k\overline{r_j r_l}) Rg\overline{M}_{\mu\nu}(k\overline{rr_j}) + A_{\mu\nu mn}(k\overline{r_j r_l}) Rg\overline{N}_{\mu\nu}(k\overline{rr_j}) \right] \tag{95}$$

where

$$A_{\mu\nu mn}(k\overline{r_j r_l}) = \frac{\gamma_{mn}}{\gamma_{\mu\nu}}(-1)^{\mu}\sum_{p=0}^{\infty} a(m,n \mid -\mu,\nu \mid p)a(n,\nu,p) \times h_p(k \mid \overline{r_j r_l} \mid) P_p^{m-\mu}(\cos\theta_{\overline{r_j r_l}})\, e^{i(m-\mu)\phi_{\overline{r_j r_l}}} \tag{96}$$

$$B_{\mu\nu mn}(k\overline{r_j r_l}) = \frac{\gamma_{mn}}{\gamma_{\mu\nu}}(-1)^{\mu+1}\sum_{p=0}^{\infty} a(m,n \mid -\mu,\nu \mid p,p-1)b(n,\nu,p) \times h_p(k \mid \overline{r_j r_l} \mid) P_p^{m-\mu}(\cos\theta_{\overline{r_j r_l}})\, e^{i(m-\mu)\phi_{\overline{r_j r_l}}} \tag{97}$$

$$\gamma_{mn} = \sqrt{\frac{(2n+1)(n-m)!}{4\pi n(n+1)(n+m)!}} \tag{98}$$

$$a(m,n \mid -\mu,\nu \mid p) = (-1)^{m+\mu}(2p+1)\sqrt{\frac{(n+m)!(\nu+\mu)!(p-m-\mu)!}{(n-m)!(\nu-\mu)!(p+m+\mu)!}} \times \begin{pmatrix} n & \nu & p \\ m & \mu & -(m+\mu) \end{pmatrix}\begin{pmatrix} n & \nu & p \\ 0 & 0 & 0 \end{pmatrix} \tag{99}$$

$$a(m,n \mid -\mu,\nu \mid p,q) = (-1)^{m+\mu}(2p+1)\sqrt{\frac{(n+m)!(\nu+\mu)!(p-m-\mu)!}{(n-m)!(\nu-\mu)!(p+m+\mu)!}} \times \begin{pmatrix} n & \nu & p \\ m & \mu & -(m+\mu) \end{pmatrix}\begin{pmatrix} n & \nu & q \\ 0 & 0 & 0 \end{pmatrix} \tag{100}$$

$$a(n,\nu,p) = \frac{(2\nu+1)}{2\nu(\nu+1)} i^{\nu-n+p}[\nu(\nu+1)+n(n+1)-p(p+1)] \tag{101}$$

$$b(n,\nu,p) = -\frac{(2\nu+1)}{2\nu(\nu+1)} i^{\nu-n+p}[(n+\nu+p+1)(\nu+p-n) \times (n+p-\nu)(n+\nu-p+1)]^{1/2} \tag{102}$$

and

$$\begin{pmatrix} j_1 & j_2 & j_3 \\ m_1 & m_2 & -(m_1+m_2) \end{pmatrix}$$

is the Wigner $3j$ symbol [33].

Equations (87), (90), (91), and (94)–(97) can be substituted into (86). To solve (86), we assume the trial solution

$$a_{\mu\nu}^{s_j}(z_j) = \alpha_{\mu\nu}^{s_j} e^{iKz_j} \tag{103}$$

$$b_{\mu\nu}^{s_j}(z_j) = \beta_{\mu\nu}^{s_j} e^{iKz_j} \tag{104}$$

where K is the effective propagation constant. Equating terms with the same $Rg\overline{M}_{\mu\nu}(k\overline{rr_j})$ and the same $Rg\overline{N}_{\mu\nu}(k\overline{rr_j})$ give the following two equations:

$$\begin{aligned}\alpha_{\mu\nu}^{s_j} e^{iKz_j} &= e^{ikz_j}\frac{i^\nu}{2}\sqrt{4\pi(2\nu+1)}\,(\delta_{\mu 1} - \delta_{\mu(-1)}) \\ &+ e^{iKz_j}\sum_{s_l=1}^{L}\sum_{n=1}^{\infty}\sum_{p=0}^{\infty} n_{s_l}(-1)^{\mu}\frac{\gamma_{\mu n}}{\gamma_{\mu\nu}}(-1)^p I_p^{s_j s_l} \\ &\times \left\{ T_n^{(M)s_l}\alpha_{\mu n}^{s_l}\, a(\mu, n \mid -\mu, \nu \mid p)\, a(n,\nu,p)\right. \\ &\left. - T_n^{(N)s_l}\beta_{\mu n}^{s_l}\, a(\mu, n \mid -\mu, \nu \mid p, p-1)\, b(n,\nu,p)\right\} \end{aligned} \tag{105}$$

$$\begin{aligned}\beta_{\mu\nu}^{s_j} e^{iKz_j} &= e^{ikz_j}\frac{i^\nu}{2}\sqrt{4\pi(2\nu+1)}\,(\delta_{\mu 1} + \delta_{\mu(-1)}) \\ &+ e^{iKz_j}\sum_{s_l=1}^{L}\sum_{n=1}^{\infty}\sum_{p=0}^{\infty} n_{s_l}(-1)^{\mu+1}\frac{\gamma_{\mu n}}{\gamma_{\mu\nu}}(-1)^p I_p^{s_j s_l} \\ &\times \left\{ T_n^{(M)s_l}\alpha_{\mu n}^{s_l}\, a(\mu, n \mid -\mu, \nu \mid p, p-1)\, b(n,\nu,p)\right. \\ &\left. - T_n^{(N)s_l}\beta_{\mu n}^{s_l}\, a(\mu, n \mid -\mu, \nu \mid p)\, a(n,\nu,p)\right\} \end{aligned} \tag{106}$$

where δ_{mn} is the Kronecker delta function and

$$I_p^{s_j s_l} = \int_{z_l \geq 0} d\overline{r}_l g_{s_j s_l}(\overline{r}_l - \overline{r}_j)\, e^{iK(z_l - z_j)} h_p(k \mid \overline{r_l r_j} \mid) P_p(\cos\theta_{\overline{r_l r_j}}) \tag{107}$$

The volume of integration of (107) consists of the half space $z_l \geq 0$ less a sphere of radius $R_{s_j s_l} = a_{s_j} + a_{s_l}$ centered at the point $\overline{r}_j$. This is due to the fact that particles do not interpenetrate each other so that $g_{s_j s_l}(\overline{r}) = 0$ for $r < R_{s_j s_l}$. We rewrite $g_{s_j s_l}(\overline{r}_l - \overline{r}_j)$ as follows

$$g_{s_j s_l}(\overline{r}_l - \overline{r}_j) = 1 + [g_{s_j s_l}(\overline{r}_l - \overline{r}_j) - 1] \tag{108}$$

so that the integral $I_p^{s_j s_l}$ in (107) can be decomposed in the following manner

$$I_p^{s_j s_l} = I_1 + I_2 \tag{109}$$

$$I_1 = \int_{|\bar{r}_l - \bar{r}_j| > R_{s_j s_l}} d\bar{r}_l \, e^{iK(z_l - z_j)} \, h_p\left(k \mid \overline{r_l r_j} \mid\right) P_p\left(\cos\theta_{\overline{r_l r_j}}\right)$$

$$= \frac{2\pi i^{p+1} e^{ikz_j}}{k^2(K-k)} e^{-iKz_j} + 4\pi i^p L_p\left(k, K \mid R_{s_j s_l}\right) \tag{110}$$

$$I_2 = \int_{|\bar{r}_l - \bar{r}_j| > R_{s_j s_l}} d\bar{r}_l \left[g_{s_j s_l}(\bar{r}_l - \bar{r}_j) - 1\right] e^{iK(z_l - z_j)}$$

$$\times h_p\left(k \mid \overline{r_l r_j} \mid\right) P_p\left(\cos\theta_{\overline{r_l r_j}}\right)$$

$$= 4\pi i^p M_p\left(k, K \mid R_{s_j s_l}\right) \tag{111}$$

where

$$L_p\left(k, K \mid R_{s_j s_l}\right) = -\frac{R^2_{s_j s_l}}{K^2 - k^2}\left[k h_p'(kR_{s_j s_l}) j_p(KR_{s_j s_l}) - K h_p(kR_{s_j s_l}) j_p'(KR_{s_j s_l})\right] \tag{112}$$

$$M_p\left(k, K \mid R_{s_j s_l}\right) = \int_{R_{s_j s_l}}^{\infty} dr r^2 \left[g_{s_j s_l}(r) - 1\right] h_p(kr) j_p(Kr) \tag{113}$$

Substituting (110) and (111) into (105) and (106) gives two types of terms in (105) and (106). One type of terms has a $\exp(ikz_j)$ dependence corresponding to waves travelling with the propagation constant of the incident wave. The terms with propagation constant k should balance each other giving the generalized Ewald–Oseen extinction theorem [8,34]. The physical interpretation is that the medium generates a wave that extinguishes the original incident wave.

$$\frac{i^\nu}{2}\sqrt{4\pi(2\nu+1)}\left(\delta_{\mu 1} - \delta_{\mu(-1)}\right)$$

$$+ \sum_{s_l=1}^{L}\sum_{n=1}^{\infty}\sum_{p=0}^{\infty} n_{s_l}(-1)^\mu (-i)^p \frac{\gamma_{\mu n}}{\gamma_{\mu\nu}} \frac{2\pi i}{k^2(K-k)}$$

$$\times \left\{ T_n^{(M)s_l} \alpha^{s_l}_{\mu n} \, a(\mu, n \mid -\mu, \nu \mid p)\, a(n, \nu, p) \right.$$

$$\left. - T_n^{(N)s_l} \beta^{s_l}_{\mu n} a(\mu, n \mid -\mu, \nu \mid p, p-1) b(n, \nu, p) \right\} = 0 \tag{114}$$

$$\frac{i^\nu}{2}\sqrt{4\pi(2\nu+1)}\left(\delta_{\mu 1} + \delta_{\mu(-1)}\right)$$

$$+ \sum_{s_l=1}^{L}\sum_{n=1}^{\infty}\sum_{p=0}^{\infty} n_{s_l}(-1)^{\mu+1} (-i)^p \frac{\gamma_{\mu n}}{\gamma_{\mu\nu}} \frac{2\pi i}{k^2(K-k)}$$

$$\times \{ T_n^{(M)s_l} \alpha_{\mu n}^{s_l} a(\mu, n \mid -\mu, \nu \mid p, p-1) b(n, \nu, p)$$
$$- T_n^{(N)s_l} \beta_{\mu n}^{s_l} a(\mu, n \mid -\mu, \nu \mid p) a(n, \nu, p)\} = 0 \qquad (115)$$

The other type of terms has an $\exp(iKz_j)$ dependence corresponding to waves travelling with the propagation constant of the effective medium. Balancing the terms with propagation constant K gives the generalized Lorentz–Lorenz law [8,34].

$$\alpha_{\mu\nu}^{s_j} = 4\pi \sum_{s_l=1}^{L} \sum_{n=1}^{\infty} \sum_{p=0}^{\infty} n_{s_l} (-1)^{\mu} (-i)^p \frac{\gamma_{\mu n}}{\gamma_{\mu\nu}}$$
$$[L_p(k, K \mid R_{s_j s_l}) + M_p(k, K \mid R_{s_j s_l})]$$
$$\times \{ T_n^{(M)s_l} \alpha_{\mu n}^{s_l} a(\mu, n \mid -\mu, \nu \mid p) a(n, \nu, p)$$
$$- T_n^{(N)s_l} \beta_{\mu n}^{s_l} a(\mu, n \mid -\mu, \nu \mid p, p-1) b(n, \nu, p)\} \qquad (116)$$

$$\beta_{\mu\nu}^{s_j} = 4\pi \sum_{s_l=1}^{L} \sum_{n=1}^{\infty} \sum_{p=0}^{\infty} n_{s_l} (-1)^{\mu+1} (-i)^p \frac{\gamma_{\mu n}}{\gamma_{\mu\nu}}$$
$$[L_p(k, K \mid R_{s_j s_l}) + M_p(k, K \mid R_{s_j s_l})]$$
$$\times \{ T_n^{(M)s_l} \alpha_{\mu n}^{s_l} a(\mu, n \mid -\mu, \nu \mid p, p-1) b(n, \nu, p)$$
$$- T_n^{(N)s_l} \beta_{\mu n}^{s_l} a(\mu, n \mid -\mu, \nu \mid p) a(n, \nu, p)\} \qquad (117)$$

The generalized Lorentz–Lorenz law provides the necessary dispersion relation for the effective propagation constant K.

On examining the generalized Ewald–Oseen extinction theorem and using the relations [8],

$$a(-\mu, n \mid \mu, \nu \mid p) = \frac{(n-\mu)!(\nu+\mu)!}{(n+\mu)!(\nu-\mu)!} a(\mu, n \mid -\mu, \nu \mid p) \qquad (118)$$

$$a(-\mu, n \mid \mu, \nu \mid p, p-1) = -\frac{(n-\mu)!(\nu+\mu)!}{(n+\mu)!(\nu-\mu)!} a(\mu, n \mid -\mu, \nu \mid p, p-1) \qquad (119)$$

it follows that $\alpha_{-1\nu}^{s_l} = -\alpha_{1\nu}^{s_l}$ and $\beta_{-1\nu}^{s_l} = \beta_{1\nu}^{s_l}$. Furthermore, by making use of the following summation identities

$$-\sum_{p=0}^{\infty} (-i)^p a(1, n \mid -1, \nu \mid p, p-1) b(n, \nu, p)$$

$$= \sum_{p=0}^{\infty} (-i)^p a(1,n \mid -1,\nu \mid p) a(n,\nu,p)$$

$$= -i^{\nu-n} \frac{(2\nu+1)n(n+1)}{2\nu(\nu+1)} \tag{120}$$

and setting

$$\alpha_{1n}^{s_l} = X_{1n}^{s_l} \frac{i^n}{2} \sqrt{4\pi(2n+1)} \tag{121}$$

$$\beta_{1n}^{s_l} = Y_{1n}^{s_l} \frac{i^n}{2} \sqrt{4\pi(2n+1)} \tag{122}$$

equations (114) and (115) of the generalized Ewald–Oseen extinction theorem can be simplified to a single equation

$$K - k = -\frac{\pi i}{k^2} \sum_{s_l=1}^{L} \sum_{n=1}^{\infty} n_{s_l} \left[T_n^{(M)s_l} X_{1n}^{s_l} + T_n^{(N)s_l} Y_{1n}^{s_l} \right] (2n+1) \tag{123}$$

Equations (116) and (117) of the generalized Lorentz–Lorenz law are also simplified to

$$\begin{aligned} X_{1\nu}^{s_j} = & -2\pi \sum_{s_l=1}^{L} \sum_{n=1}^{\infty} \sum_{p=0}^{\infty} n_{s_l} (2n+1) \\ & \left[L_p\left(k, K \mid R_{s_j s_l}\right) + M_p\left(k, K \mid R_{s_j s_l}\right) \right] \\ & \times \left\{ T_n^{(M)s_l} X_{1n}^{s_l} a(1,n \mid -1,\nu \mid p) A(n,\nu,p) \right. \\ & \left. + T_n^{(N)s_l} Y_{1n}^{s_l} a(1,n \mid -1,\nu \mid p,p-1) B(n,\nu,p) \right\} \end{aligned} \tag{124}$$

$$\begin{aligned} Y_{1\nu}^{s_j} = & -2\pi \sum_{s_l=1}^{L} \sum_{n=1}^{\infty} \sum_{p=0}^{\infty} n_{s_l} (2n+1) \\ & \left[L_p\left(k, K \mid R_{s_j s_l}\right) + M_p\left(k, K \mid R_{s_j s_l}\right) \right] \\ & \times \left\{ T_n^{(M)s_l} X_{1n}^{s_l} a(1,n \mid -1,\nu \mid p,p-1) B(n,\nu,p) \right. \\ & \left. + T_n^{(N)s_l} Y_{1n}^{s_l} a(1,n \mid -1,\nu \mid p) A(n,\nu,p) \right\} \end{aligned} \tag{125}$$

where

$$A(n,\nu,p) = \frac{\nu(\nu+1) + n(n+1) - p(p+1)}{n(n+1)} \tag{126}$$

$$B(n,\nu,p) = \frac{\sqrt{(n+\nu+p+1)(\nu+p-n)(n+p-\nu)(n+\nu-p+1)}}{n(n+1)} \tag{127}$$

Equations (124) and (125) form a system of simultaneous homogeneous equations for the unknowns $X_{1n}^{s_l}$ and $Y_{1n}^{s_l}$. For a nontrivial solution, the determinant of the coefficients must vanish. The requirement for the vanishing of the determinant gives an equation for the effective wavenumber K. Thus, for given particle sizes a_{s_l}, number densities n_{s_j}, and permittivities ϵ_{s_l}, $s_l = 1,2,\ldots,L$, we calculate the Mie scattering coefficients $T_n^{(M)s_l}$ and $T_n^{(N)s_l}$, the pair distribution functions $g_{s_j s_l}(\bar{r})$, and the expressions $L_p\left(k, K \mid R_{s_j s_l}\right)$ and $M_p\left(k, K \mid R_{s_j s_l}\right)$. The effective propagation constant K is then calculated by searching it in the complex plane such that the determinant of equations (124)–(125) will vanish.

In the following, we summarize the numerical algorithm that we used to compute the effective propagation constant K. For the values of ka up to 2.5, and L species of particles, the determinant of the coefficients of $X_{1\nu}^{s_j}$ and $Y_{1\nu}^{s_j}$ is computed numerically by retaining a maximum of $12 \cdot L$ simultaneous homogeneous equations for $X_{1\nu}^{s_l}$ and $Y_{1\nu}^{s_l}$, $\nu = 1,2,\ldots,6; s_l = 1,2,\ldots,L$. The Wigner $3j$ symbols are generated by a computer code. The elements of $M_p\left(k, K \mid R_{s_j s_l}\right)$ for $p = 0,1,\ldots,12$ were computed by numerically evaluating the integral in (113) for r between $R_{s_j s_l}$ and $5R_{s_j s_l}$, the value of $g_{s_j s_l}(r) - 1$ is assumed to be zero for r larger than $5R_{s_j s_l}$.

For the given values of ka_{s_j} and f_{s_j}, the roots of the determinant were searched in the complex K plane $(K_r + iK_i)$ using Muller's method. We have used two good initial guesses. One initial guess is provided by the low frequency solution for the effective propagation constant under quasicrystalline approximation of (69). The other good initial guess is the result under Foldy's approximation obtained by replacing $X_{1n}^{s_j}$ and $Y_{1n}^{s_j}$ by 1 in (123)

$$K^{(F)} = k - \frac{\pi i}{k^2} \sum_{s_l=1}^{L} \sum_{n=1}^{\infty} n_{s_l} \left[T_n^{(M)s_l} + T_n^{(N)s_l}\right] (2n+1) \tag{128}$$

where $K^{(F)}$ denotes the effective propagation constant under Foldy's approximation. These two guesses could be used systematically to obtain quick convergence of roots at increasing higher values of ka_{s_j}. In the following, we shall present the results for the normalized phase velocity k/K_r and the effective loss tangent $2K_i/K_r$. The effective loss tangent accounts for attenuation due to both scattering and absorption.

In Figs. 3.5.2–3.5.5, we illustrate the effective propagation constant for the case when the particles are of identical sizes. In Figs. 3.5.2 and 3.5.3, the normalized phase velocity and the effective loss tangent are plotted as a function of ka for $f = 0.1$ and $f = 0.2$. The results for the case of lossless particles, $\epsilon = 3.2\epsilon_o$, and the case of lossy particles, $\epsilon = (3.2 + i0.15)\epsilon_o$, are also illustrated. We note that the phase velocity first decreases with increasing particle size and oscillates as particle size increases further. The oscillation is a characteristic of resonant scattering for large particles. Comparing the loss tangents for the two cases of lossy and lossless particles, we note that, for small particles, absorption dominates over scattering as the effective loss tangent for lossy case is much larger than that for lossless case. For ka up to 2.5, the loss tangents are comparable in magnitude in the two cases. In Figs. 3.5.4 and 3.5.5, we show respectively phase velocity and loss tangent versus f for $ka = 1.5$ and $ka = 2$ with $\epsilon = 3.2\epsilon_o$. We note that the phase velocity decreases as f increases since the phase velocity for the scatterers is lower. As a function of f, the effective loss tangent first increases, then rises to a peak and decreases as f further increases. This indicates that the medium appears more homogeneous as f further increases beyond a certain value.

In Figs. 3.5.6–3.5.9, we illustrate the case when the particles are of two different sizes. In Figs. 3.5.6 and 3.5.7, the normalized phase velocity and the effective loss tangent are plotted as a function of ka_2 for $f_2 = 0.1$ and $f_2 = 0.2$ with $ka_1 = 0.5$ and $f_1 = 0.1$. The results for the case of lossless particles, $\epsilon_1 = \epsilon_2 = 3.2\epsilon_o$, and the case of lossy particles, $\epsilon_1 = \epsilon_2 = (3.2 + i0.15)\epsilon_o$, are illustrated. In Figs. 3.5.8 and 3.5.9, we show respectively phase velocity and loss tangent vs f_2 for $ka_2 = 1.5$ and $ka_2 = 2$ with $ka_1 = 0.5$, $f_1 = 0.1$, and $\epsilon_1 = \epsilon_2 = 3.2\epsilon_o$. We see that the location of maximum attenuation occurs at a larger f_2 for the case of larger ka. This indicates that independent scattering has a wider regime of validity for larger particles.

In Figs. 3.5.10–3.5.13, we illustrate the case when there are four species of particles represented by four different sizes. In Figs. 3.5.10 and 3.5.11, the normalized phase velocity and the effective loss tangent are plotted as a function of ka_4 for $f_4 = 0.05$ and $f_4 = 0.1$ with $ka_1 = 0.2$, $ka_2 = 0.3$, $ka_3 = 0.5$ and $f_1 = 0.1$, $f_2 = 0.15$, and $f_3 = 0.05$. We also compare the results for the lossless particle case, $\epsilon_1 = \epsilon_2 = \epsilon_3 = \epsilon_4 = 3.2\epsilon_o$ and the lossy particle case, $\epsilon_1 = \epsilon_2 = \epsilon_3 = \epsilon_4 = (3.2 + i0.15)\epsilon_o$. Figs. 3.5.12 and 3.5.13 plot respectively the phase

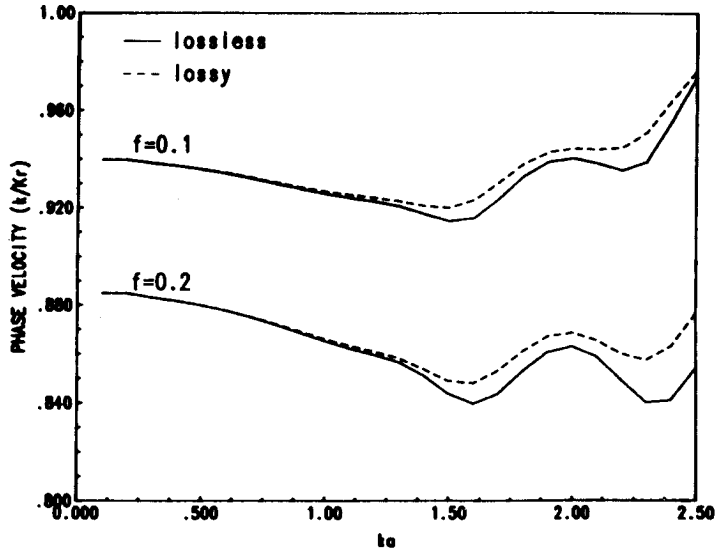

Figure 3.5.2 Normalized phase velocity k/K_r as a function of ka for (1)$f = 0.1$ and (2)$f = 0.2$. The results of lossless particles, $\epsilon = 3.2\epsilon_o$, and of lossy particles, $\epsilon = (3.2 + i0.15)\epsilon_o$, are illustrated.

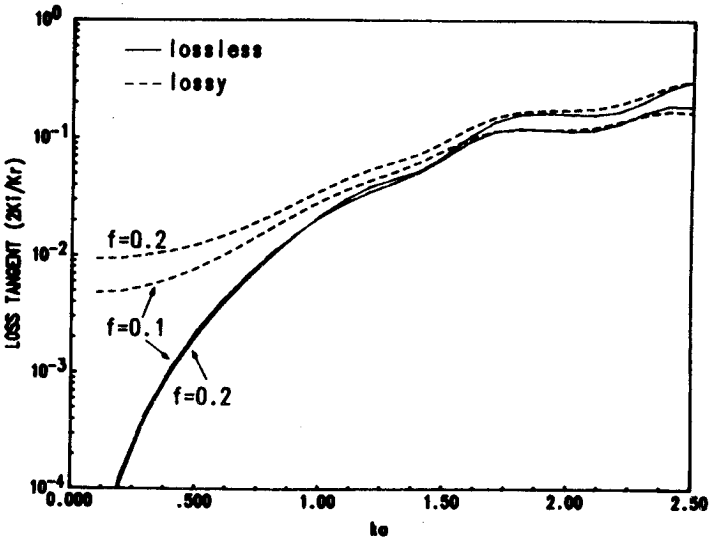

Figure 3.5.3 Effective loss tangent $2K_i/K_r$ as a function of ka for (1)$f = 0.1$ and (2)$f = 0.2$. The results of lossless particles, $\epsilon = 3.2\epsilon_o$, and of lossy particles, $\epsilon = (3.2 + i0.15)\epsilon_o$, are illustrated.

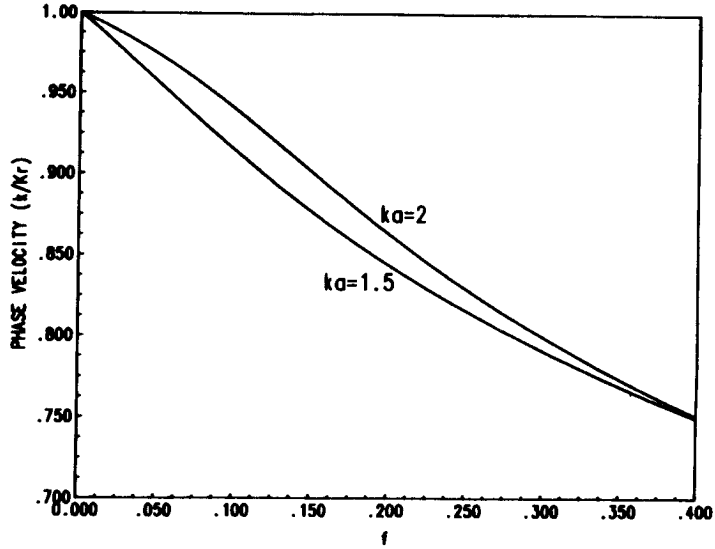

Figure 3.5.4 Normalized phase velocity k/K_r as a function of f for $(1)ka = 1.5$ and $(2)ka = 2$, and $\epsilon = 3.2\epsilon_o$.

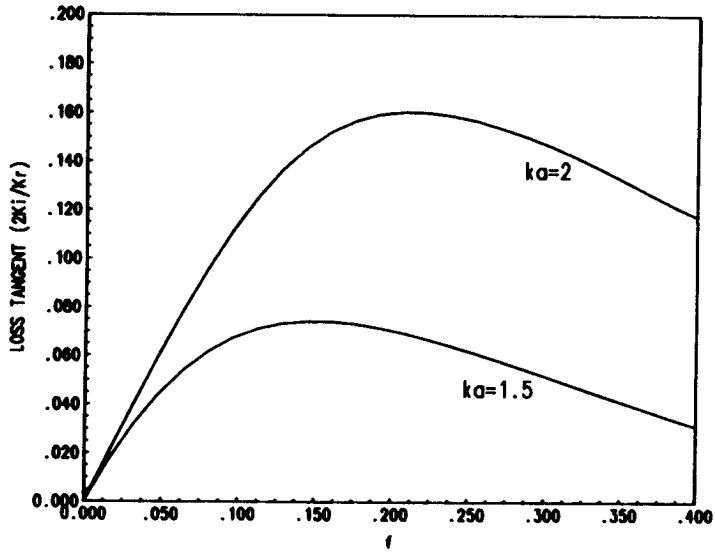

Figure 3.5.5 Effective loss tangent $2K_i/K_r$ as a function of f for $(1)ka = 1.5$ and $(2)ka = 2$, and $\epsilon = 3.2\epsilon_o$.

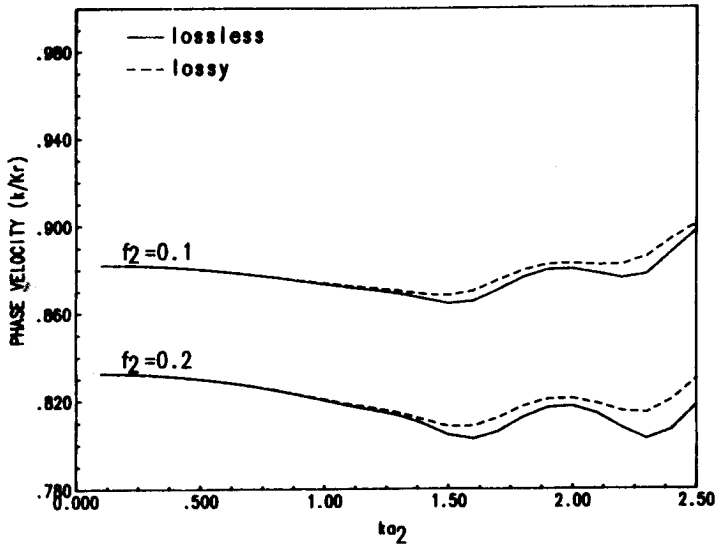

Figure 3.5.6 Normalized phase velocity k/K_r as a function of ka_2 for u $(1)f_2 = 0.1$ and $(2)f_2 = 0.2$, where $ka_1 = 0.5$ and $f_1 = 0.1$. The results of lossless particles, $\epsilon_1 = \epsilon_2 = 3.2\epsilon_o$, and of lossy particles, $\epsilon_1 = \epsilon_2 = (3.2 + i0.15)\epsilon_o$, are illustrated.

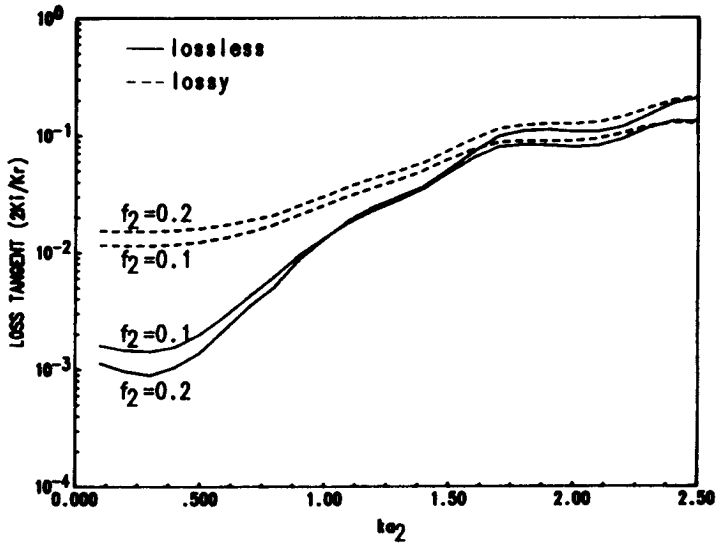

Figure 3.5.7 Effective loss tangent $2K_i/K_r$ as a function of ka_2 for $(1)f_2 = 0.1$ and $(2)f_2 = 0.2$, where $ka_1 = 0.5$ and $f_1 = 0.1$. The results of lossless particles, $\epsilon_1 = \epsilon_2 = 3.2\epsilon_o$, and of lossy particles, $\epsilon_1 = \epsilon_2 = (3.2 + i0.15)\epsilon_o$, are illustrated.

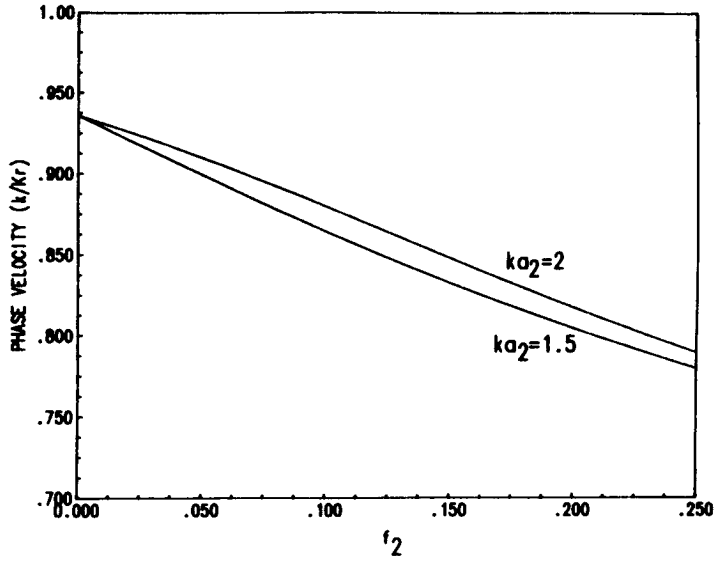

Figure 3.5.8 Normalized phase velocity k/K_r as a function of f_2 for (1)$ka_2 = 1.5$ and (2)$ka_2 = 2$, where $ka_1 = 0.5$ and $f_1 = 0.1$ and $\epsilon_1 = \epsilon_2 = 3.2\epsilon_o$.

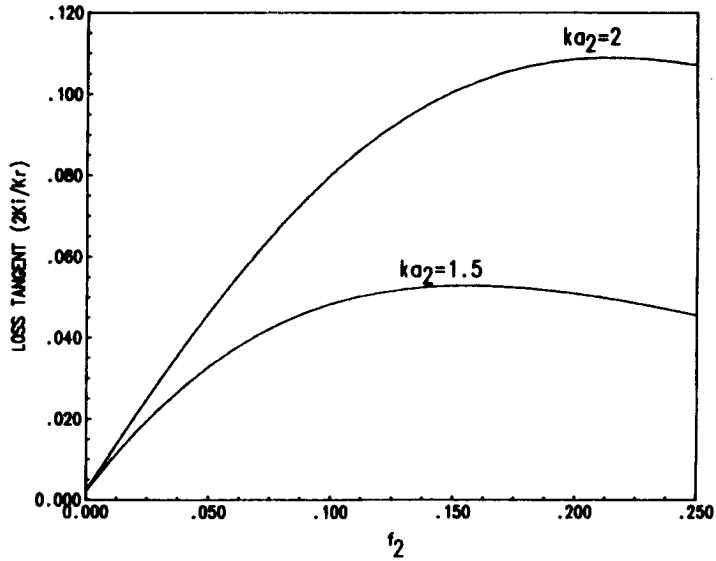

Figure 3.5.9 Effective loss tangent $2K_i/K_r$ as a function of f_2 for (1)$ka_2 = 1.5$ and (2)$ka_2 = 2$, where $ka_1 = 0.5$ and $f_1 = 0.1$ and $\epsilon_1 = \epsilon_2 = 3.2\epsilon_o$.

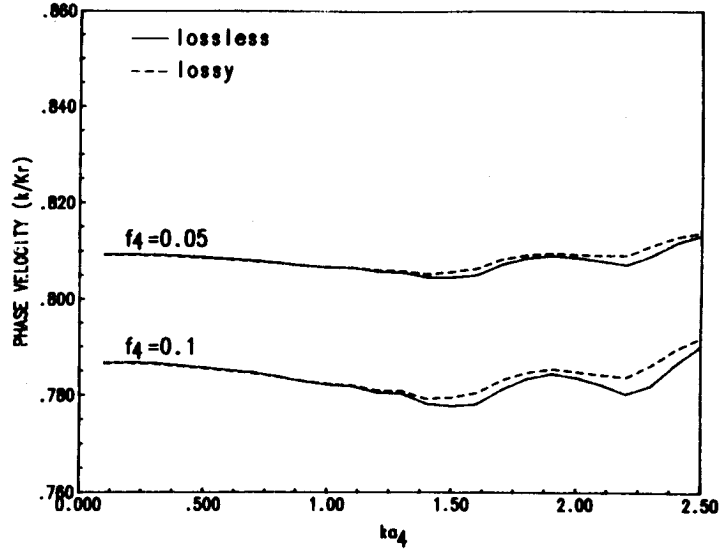

Figure 3.5.10 Normalized phase velocity k/K_r as a function of ka_4 for (1)$f_4 = 0.05$ and (2)$f_4 = 0.1$, where $ka_1 = 0.2$, $ka_2 = 0.3$, $ka_3 = 0.5$ and $f_1 = 0.1$, $f_2 = 0.15$, $f_3 = 0.05$. The results of lossless particles, $\epsilon_1 = \epsilon_2 = \epsilon_3 = \epsilon_4 = 3.2\epsilon_o$, and of lossy particles, $\epsilon_1 = \epsilon_2 = \epsilon_3 = \epsilon_4 = (3.2 + i0.15)\epsilon_o$, are illustrated.

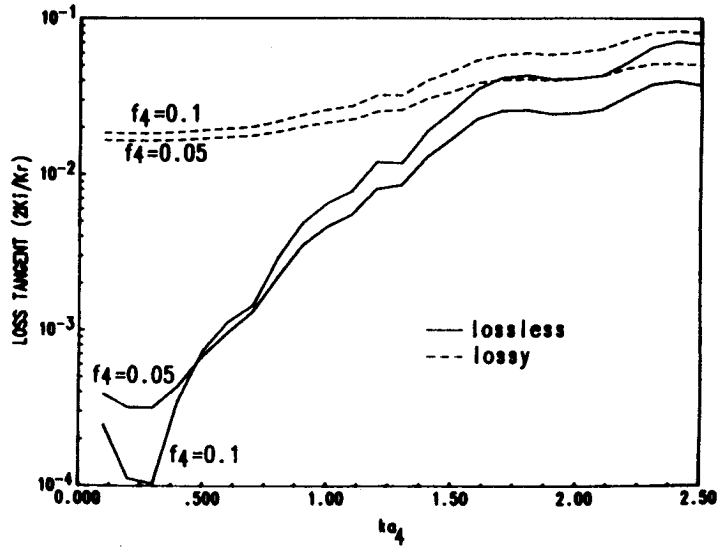

Figure 3.5.11 Effective loss tangent $2K_i/K_r$ as a function of ka_4 for (1)$f_4 = 0.05$ and (2)$f_4 = 0.1$, where $ka_1 = 0.2$, $ka_2 = 0.3$, $ka_3 = 0.5$ and $f_1 = 0.1$, $f_2 = 0.15$, $f_3 = 0.05$. The results of lossless particles, $\epsilon_1 = \epsilon_2 = \epsilon_3 = \epsilon_4 = 3.2\epsilon_o$, and of lossy particles, $\epsilon_1 = \epsilon_2 = \epsilon_3 = \epsilon_4 = (3.2 + i0.15)\epsilon_o$, are illustrated.

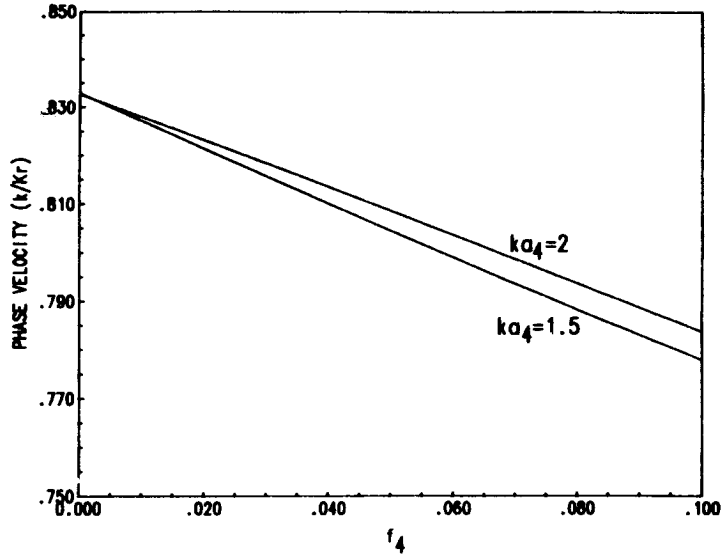

Figure 3.5.12 Normalized phase velocity k/K_r as a function of f_4 for (1)$ka_4 = 1.5$ and (2)$ka_4 = 2$, where $ka_1 = 0.2$, $ka_2 = 0.3$, $ka_3 = 0.5$, $f_1 = 0.1$, $f_2 = 0.15$, $f_3 = 0.05$, and $\epsilon_1 = \epsilon_2 = \epsilon_3 = \epsilon_4 = 3.2\epsilon_o$.

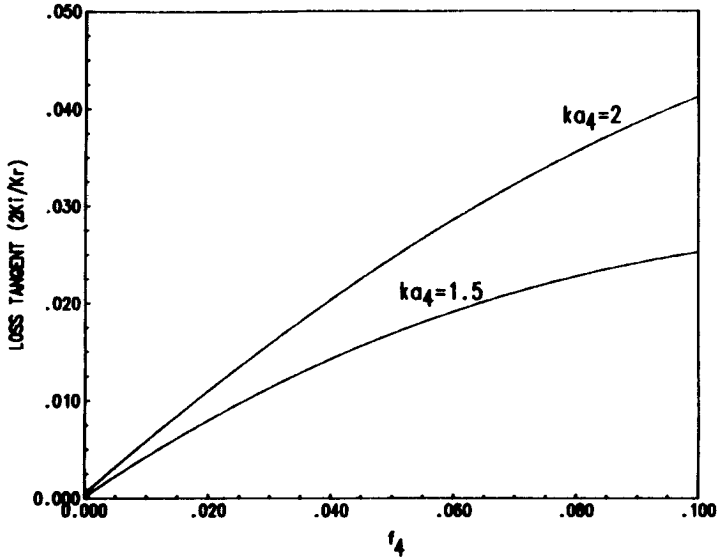

Figure 3.5.13 Effective loss tangent $2K_i/K_r$ as a function of f_4 for (1)$ka_4 = 1.5$ and (2)$ka_4 = 2$, where $ka_1 = 0.2$, $ka_2 = 0.3$, $ka_3 = 0.5$, $f_1 = 0.1$, $f_2 = 0.15$, $f_3 = 0.05$, and $\epsilon_1 = \epsilon_2 = \epsilon_3 = \epsilon_4 = 3.2\epsilon_o$.

velocity and the loss tangent as a function of f_4 for $ka_4 = 1.5$ and $ka_4 = 2$ with $ka_1 = 0.2$, $ka_2 = 0.3$, $ka_3 = 0.5$, $f_1 = 0.1$, $f_2 = 0.15$, $f_3 = 0.05$, and $\epsilon_1 = \epsilon_2 = \epsilon_3 = \epsilon_4 = 3.2\epsilon_o$.

We have shown the numerical results for the cases of one, two and four different species. The numerical algorithm can be extended to more number of species.

3.6 Energy Conservation and Ladder Approximation for Dense Media with Multiple Species

In multiple scattering of waves in lossless media or slightly lossy media, one important problem is to calculate the second moment of the incoherent fields (such a problem is often neglected for media of moderate loss or for cases of extremely long wavelengths). A common approximation to the Bethe–Salpeter equation of the second moment is the ladder approximation. The second moment equation also utilizes the first moment Green's function and the first moment of the field. Thus, the result of the second moment and the question of energy conservation depends on the choices of approximations for the first moment equation as well as that for the second moment equation. A test of energy conservation is provided by the integrated optical relation [8].

In the following, we shall show that the ladder approximation and the quasicrystalline approximation with coherent potential satisfy the integrated optical relation exactly. In the process, we have also derived the ladder approximation for dense medium with multiple species of particles taking into account the effect of correlated scatterers.

The time-averaged Poynting's vector $\overline{S}$ is defined as

$$\overline{S} = \frac{1}{4i\omega\mu}\left\{-\overline{E} \times \left(\overline{\nabla} \times \overline{E^*}\right) + \overline{E^*} \times \left(\overline{\nabla} \times \overline{E}\right)\right\} \tag{129}$$

We also use angular bracket to denote ensemble average. The integrated optical relation states that, for lossless background and particles, the integration over space of the divergence of the time averaged Poynting's vector must be zero.

$$\int d\overline{r}\, \langle \overline{\nabla} \cdot \overline{S} \rangle = 0 \tag{130}$$

The vector wave equation governing the electric field is

$$\overline{E}(\bar{r}) = \overline{E}^{inc}(\bar{r}) + \sum_{l=1}^{N} \int d\bar{r}' \overline{\overline{G}}_o(\bar{r},\bar{r}') U_l'^{l}(\bar{r}') \overline{E}(\bar{r}') \tag{131}$$

Let the operator $\overline{\overline{W}}$ be defined by

$$\overline{\overline{W}}(\bar{r}) \cdot \overline{E}(\bar{r}) = \overline{\nabla} \times \overline{\nabla} \times \overline{E}(\bar{r}) - k^2 \overline{E}(\bar{r}) \tag{132}$$

so that

$$\overline{\overline{W}}(\bar{r}) \cdot \overline{E}(\bar{r}) = \sum_{l=1}^{N} U_l'^{l}(\bar{r}) \overline{E}(\bar{r}) \tag{133}$$

The integrated optical relation of (130), by using (129), (133), and the fact that $U_l'^{l}$ is real for lossless scatterers, assumes the form

$$4i\omega\mu \int d\bar{r} \langle \overline{\nabla} \cdot \overline{S}(\bar{r}) \rangle = \int d\bar{r} \sum_{\alpha,\beta} \lim_{\bar{r}' \to \bar{r}} \Big\{ W_{\alpha\beta}(\bar{r}') \langle E_\alpha(\bar{r}) E_\beta^*(\bar{r}') \rangle - W_{\alpha\beta}(\bar{r}) \langle E_\beta(\bar{r}) E_\alpha^*(\bar{r}') \rangle \Big\} \tag{134}$$

In (134), the Greek index subscripts $\alpha, \beta = 1, 2, 3$ are used to denote the Cartesian field components.

The coherent field $\langle \overline{E}(\bar{r}) \rangle$ and the coherent Green's function both obey the Dyson's equation [8,17]

$$\overline{\nabla} \times \overline{\nabla} \times \langle \overline{E}(\bar{r}) \rangle - k^2 \langle \overline{E}(\bar{r}) \rangle = \int d\bar{r}' \overline{\overline{M}}(\bar{r},\bar{r}') \cdot \langle \overline{E}(\bar{r}') \rangle \tag{135}$$

$$\overline{\nabla} \times \overline{\nabla} \times \left\langle \overline{\overline{G}}(\bar{r},\bar{r}') \right\rangle - k^2 \left\langle \overline{\overline{G}}(\bar{r},\bar{r}') \right\rangle = \overline{\overline{I}} \delta(\bar{r} - \bar{r}') + \int d\bar{r}'' \overline{\overline{M}}(\bar{r},\bar{r}'') \cdot \left\langle \overline{\overline{G}}(\bar{r}'',\bar{r}') \right\rangle \tag{136}$$

where $\overline{\overline{M}}$ is the mass operator. Equations (135) and (136) are generally true and the exact mass operator contains an infinite number of terms. Comparisons with (28) and (41) of section 3.2 show that the QCA and QCA–CP can be cast in the form of (135) and (136). Thus, (26) and

(37) give the approximations for the mass operator under QCA and QCA–CP respectively.

Generally, the second moment of the field obeys the Bethe–Salpeter equation [8,17]

$$\begin{aligned}\langle E_\alpha(\bar{r})\ E^*_\beta(\bar{r}')\rangle &= \langle E_\alpha(\bar{r})\rangle\langle E^*_\beta(\bar{r}')\rangle \\ &+ \sum_{\alpha',\beta'}\sum_{\alpha'',\beta''}\int d\bar{r}_1\int d\bar{r}_2\int d\bar{r}'_1\int d\bar{r}'_2 \\ &\cdot\langle G_{\alpha\alpha'}(\bar{r},\bar{r}_1)\rangle\langle G^*_{\beta\beta'}(\bar{r}',\bar{r}'_1)\rangle \\ &\cdot I_{\alpha'\alpha'';\beta'\beta''}(\bar{r}_1,\bar{r}_2;\bar{r}'_1,\bar{r}'_2)\langle E_{\alpha''}(\bar{r}_2)\,E^*_{\beta''}(\bar{r}'_2)\rangle \qquad (137)\end{aligned}$$

From (135)–(137), it follows that

$$\begin{aligned}&\sum_\beta W_{\alpha\beta}(\bar{r}')\langle E_\alpha(\bar{r})\,E^*_\beta(\bar{r}')\rangle = \\ &\langle E_\alpha(\bar{r})\rangle\sum_\beta\int d\bar{r}_2 M^*_{\alpha\beta}(\bar{r}',\bar{r}_2)\langle E^*_\beta(\bar{r}_2)\rangle \\ &+\sum_{\alpha'}\sum_{\alpha'',\beta''}\int d\bar{r}_1\int d\bar{r}_2\int d\bar{r}'_2\langle G_{\alpha\alpha'}(\bar{r},\bar{r}_1)\rangle \\ &\cdot I_{\alpha'\alpha'';\alpha\beta''}(\bar{r}_1,\bar{r}_2;\bar{r}',\bar{r}'_2)\langle E_{\alpha''}(\bar{r}_2)\,E^*_{\beta''}(\bar{r}'_2)\rangle \\ &+\sum_\beta\sum_{\alpha',\beta'}\sum_{\alpha'',\beta''}\int d\bar{r}_1\int d\bar{r}_2\int d\bar{r}'_1\int d\bar{r}'_2\langle G_{\alpha\alpha'}(\bar{r},\bar{r}_1)\rangle \\ &\cdot\int d\bar{r}''_2 M^*_{\alpha\beta}(\bar{r}',\bar{r}''_2)\langle G^*_{\beta\beta'}(\bar{r}''_2,\bar{r}'_1)\rangle \\ &\cdot I_{\alpha'\alpha'';\beta'\beta''}(\bar{r}_1,\bar{r}_2;\bar{r}'_1,\bar{r}'_2)\langle E_{\alpha''}(\bar{r}_2)\,E^*_{\beta''}(\bar{r}'_2)\rangle \qquad (138)\end{aligned}$$

Next apply the Bethe–Salpeter equation of (137) to the second term on the right hand side of (138). This gives

$$\begin{aligned}&\sum_\beta W_{\alpha\beta}(\bar{r}')\langle E_\alpha(\bar{r})\,E^*_\beta(\bar{r}')\rangle = \\ &\langle E_\alpha(\bar{r})\rangle\sum_\beta\int d\bar{r}_2 M^*_{\alpha\beta}(\bar{r}',\bar{r}_2)\langle E^*_\beta(\bar{r}_2)\rangle \\ &+\sum_{\alpha'}\sum_{\alpha'',\beta''}\int d\bar{r}_1\int d\bar{r}_2\int d\bar{r}'_2\langle G_{\alpha\alpha'}(\bar{r},\bar{r}_1)\rangle\end{aligned}$$

$$\cdot I_{\alpha'\alpha'';\alpha\beta''}(\bar{r}_1,\bar{r}_2;\bar{r}',\bar{r}'_2)\langle E_{\alpha''}(\bar{r}_2)\rangle\langle E^*_{\beta''}(\bar{r}'_2)\rangle$$

$$+\sum_{\alpha'}\sum_{\alpha'',\beta''}\int d\bar{r}_1\int d\bar{r}_2\int d\bar{r}'_2\langle G_{\alpha\alpha'}(\bar{r},\bar{r}_1)\rangle I_{\alpha'\alpha'';\alpha\beta''}(\bar{r}_1,\bar{r}_2;\bar{r}',\bar{r}'_2)$$

$$\cdot\sum_{\alpha_1,\beta_1}\sum_{\alpha_2,\beta_2}\int d\bar{r}_3\int d\bar{r}_4\int d\bar{r}'_3\int d\bar{r}'_4\langle G_{\alpha''\alpha_1}(\bar{r}_2,\bar{r}_3)\rangle$$

$$\cdot\langle G^*_{\beta''\beta_1}(\bar{r}'_2,\bar{r}'_3)\rangle I_{\alpha_1\alpha_2;\beta_1\beta_2}(\bar{r}_3,\bar{r}_4;\bar{r}'_3,\bar{r}'_4)\langle E_{\alpha_2}(\bar{r}_4)E^*_{\beta_2}(\bar{r}'_4)\rangle$$

$$+\sum_{\beta}\sum_{\alpha',\beta'}\sum_{\alpha'',\beta''}\int d\bar{r}_1\int d\bar{r}_2\int d\bar{r}'_1\int d\bar{r}'_2\langle G_{\alpha\alpha'}(\bar{r},\bar{r}_1)\rangle$$

$$\cdot\int d\bar{r}''_2 M^*_{\alpha\beta}(\bar{r}',\bar{r}''_2)\langle G^*_{\beta\beta'}(\bar{r}''_2,\bar{r}'_1)\rangle$$

$$\cdot I_{\alpha'\alpha'';\beta'\beta''}(\bar{r}_1,\bar{r}_2;\bar{r}'_1,\bar{r}'_2)\langle E_{\alpha''}(\bar{r}_2)E^*_{\beta''}(\bar{r}'_2)\rangle \qquad (139)$$

Similar manipulation can be applied to $\sum_{\beta} W_{\alpha\beta}(\bar{r})\langle E^*_{\alpha}(\bar{r}')E_{\beta}(\bar{r})\rangle$. The result expression and (139) are then substituted into the right hand side of equation (134). The limit $\bar{r}' \longrightarrow \bar{r}$ is taken and the integration is carried out over $d\bar{r}$. There are eight terms. By interchanging dummy indices and arguments, the eight terms can be rearranged, factorized and cast into the following form

$$4i\omega\mu\int d\bar{r}\langle\bar{\nabla}\cdot\bar{S}(\bar{r})\rangle =$$

$$\int d\bar{r}_2\int d\bar{r}'_2\sum_{\alpha'',\beta''}\{M^*_{\alpha''\beta''}(\bar{r}_2,\bar{r}'_2)-M_{\beta''\alpha''}(\bar{r}'_2,\bar{r}_2)$$

$$+\int d\bar{r}\int d\bar{r}_1\sum_{\alpha,\alpha''}[\langle G_{\alpha\alpha'}(\bar{r},\bar{r}_1)\rangle-\langle G^*_{\alpha'\alpha}(\bar{r}_1,\bar{r})\rangle]$$

$$\cdot I_{\alpha'\alpha'';\alpha\beta''}(\bar{r}_1,\bar{r}_2;\bar{r},\bar{r}'_2)\}\langle E_{\alpha''}(\bar{r}_2)\rangle\langle E^*_{\beta''}(\bar{r}'_2)\rangle$$

$$+\sum_{\alpha_1\beta_1}\sum_{\alpha_2,\beta_2}\sum_{\alpha'',\beta''}\int d\bar{r}_2\int d\bar{r}_3\int d\bar{r}_4\int d\bar{r}'_3\int d\bar{r}'_4\int d\bar{r}'_2$$

$$\cdot\langle G_{\alpha''\alpha_1}(\bar{r}_2,\bar{r}_3)\rangle\langle G^*_{\beta''\beta_1}(\bar{r}'_2,\bar{r}'_3)\rangle$$

$$\cdot I_{\alpha_1\alpha_2;\beta_1\beta_2}(\bar{r}_3,\bar{r}_4;\bar{r}'_3,\bar{r}'_4)\langle E_{\alpha_2}(\bar{r}_4)E^*_{\beta_2}(\bar{r}'_4)\rangle$$

$$\cdot\left\{M^*_{\alpha''\beta''}(\bar{r}_2,\bar{r}'_2)-M_{\beta''\alpha''}(\bar{r}'_2,\bar{r}_2)+\int d\bar{r}_1\sum_{\alpha,\alpha'}\int d\bar{r}\right.$$

$$\cdot\left[\langle G_{\alpha\alpha'}(\bar{r},\bar{r}_1)\rangle - \langle G^*_{\alpha'\alpha}(\bar{r}_1,\bar{r})\rangle\right] I_{\alpha'\alpha'';\alpha\beta''}(\bar{r}_1,\bar{r}_2;\bar{r},\bar{r}_2')\Big\} \quad (140)$$

From (140), it follows that the integrated optical relation is satisfied exactly if

$$M^*_{\alpha\beta}(\bar{r},\bar{r}') - M_{\beta\alpha}(\bar{r}',\bar{r}) + \sum_{\alpha',\beta'}\int d\bar{r}_1 \int d\bar{r}_2$$
$$\cdot\left[\langle G_{\alpha'\beta'}(\bar{r}_1,\bar{r}_2)\rangle - \langle G^*_{\beta'\alpha'}(\bar{r}_2,\bar{r}_1)\rangle\right] I_{\beta'\alpha;\alpha'\beta}(\bar{r}_2,\bar{r};\bar{r}_1,\bar{r}') = 0 \quad (141)$$

In the following we shall show that the condition is obeyed by QCA–CP and the ladder approximation that is modified for dense medium. From (37), the mass operator under QCA–CP is $\overline{\overline{\widehat{M}}}$ which

$$\overline{\overline{\widehat{M}}} = \sum_{s_j=1}^{L} n_{s_j} \int d\bar{r}_j \overline{\overline{\widehat{C}}}^{s_j}_j \quad (142)$$

Let superscript $\dagger$ denote Hermitian adjoint such that

$$\left(\overline{\overline{A}}^{\dagger}\right)_{\alpha''\beta''}(\bar{r}_2,\bar{r}_2') = \overline{\overline{A}}^{*}_{\beta''\alpha''}(\bar{r}_2',\bar{r}_2) \quad (143)$$

It follows from (33) and (38) that

$$\overline{\overline{\widehat{C}}}^{s_j}_j = \overline{\overline{U}}^{s_j}_j + \sum_{s_l=1}^{L}\int d\bar{r}_l q_{s_j s_l}(\bar{r}_j - \bar{r}_l)\overline{\overline{U}}^{s_j}_j \overline{\overline{G}}_c \overline{\overline{\widehat{C}}}^{s_l}_l \quad (144)$$

where

$$q_{s_j s_l}(\bar{r}_j - \bar{r}_l) = \delta_{s_j s_l}\delta(\bar{r}_j - \bar{r}_l) + n_{s_l} h_{s_j s_l}(\bar{r}_j - \bar{r}_l) \quad (145)$$

From (142), (144), and

$$\overline{\overline{U}}^{s_j\dagger}_j = \overline{\overline{U}}^{s_j}_j \quad (146)$$

for lossless scatterers, it follows that

$$\overline{\overline{\widehat{M}}}^{\dagger} - \overline{\overline{\widehat{M}}} = \sum_{s_j=1}^{L}\sum_{s_l=1}^{L} n_{s_j}\int d\bar{r}_j \int d\bar{r}_l\, q_{s_j s_l}(\bar{r}_j - \bar{r}_l)$$
$$\cdot\left[\overline{\overline{\widehat{C}}}^{s_l\dagger}_l \overline{\overline{G}}^{\dagger}_c \overline{\overline{U}}^{s_j}_j - \overline{\overline{U}}^{s_j}_j \overline{\overline{G}}_c \overline{\overline{\widehat{C}}}^{s_l}_l\right] \quad (147)$$

Next, use $\overline{\overline{U}}_j^{s_j}$ from (144) to substitute in the first $\overline{\overline{U}}_j^{s_j}$ in (147). For the second $\overline{\overline{U}}_j^{s_j}$ in (147), use

$$\overline{\overline{U}}_j^{s_j} = \overline{\overline{\widehat{C}}}_j^{s_j\dagger} - \sum_{s_m=1}^{L} \int d\bar{r}_m q_{s_j s_m}(\bar{r}_j - \bar{r}_m) \overline{\overline{\widehat{C}}}_m^{s_m\dagger} \overline{\overline{G}}_c^{\dagger} \overline{\overline{U}}_j^{s_j} \tag{148}$$

which is a consequence of (144) and (146). Thus, we get four terms in the right hand side of (147). Two of the terms cancel on exchange of dummy indices and arguments. The result is

$$\overline{\overline{\widehat{M}}}^{\dagger} - \overline{\overline{\widehat{M}}} = \sum_{s_j=1}^{L} \sum_{s_l=1}^{L} n_{s_j} \int d\bar{r}_j \int d\bar{r}_l\, q_{s_j s_l}(\bar{r}_j - \bar{r}_l) \cdot \left[\overline{\overline{\widehat{C}}}_l^{s_l\dagger} \overline{\overline{G}}_c^{\dagger} \overline{\overline{\widehat{C}}}_j^{s_j} - \overline{\overline{\widehat{C}}}_j^{s_j\dagger} \overline{\overline{G}}_c \overline{\overline{\widehat{C}}}_l^{s_l} \right] \tag{149}$$

Since $h_{s_j s_l}(\bar{r}_j - \bar{r}_l)$ is symmetric with respect to s_j and s_l as well as $\bar{r}_j$ and $\bar{r}_l$, it follows that $n_{s_j} q_{s_j s_l}(\bar{r}_j - \bar{r}_l) = n_{s_l} q_{s_l s_j}(\bar{r}_j - \bar{r}_l)$. Thus (149) is of the same form as the requirement of energy conservation of (141) provided that the intensity operator is chosen as

$$I_{\alpha\beta;\alpha'\beta'}(\bar{r}, \bar{r}_1; \bar{r}', \bar{r}_1') = \sum_{s_j=1}^{L} \sum_{s_l=1}^{L} \int d\bar{r}_j \int d\bar{r}_l \left[n_{s_j} \delta_{s_j s_l} \delta(\bar{r}_j - \bar{r}_l) + n_{s_j} n_{s_l} h_{s_j s_l}(\bar{r}_j - \bar{r}_l) \right] \widehat{C}_{l\alpha\beta}^{s_l}(\bar{r}, \bar{r}_1) \widehat{C}_{j\alpha'\beta'}^{s_j *}(\bar{r}', \bar{r}_1') \tag{150}$$

The intensity operator represents a sum of contribution form the same scatterer as represented by the first term in (150) and from different scatterers weighted by $n_{s_j} n_{s_l} h_{s_j s_l}(\bar{r}_j - \bar{r}_l)$ as represented by the second term in (150). As noted in the previous sections, $\overline{\overline{\widehat{C}}}_j^{s_j}$ represents transition scattering matrix of the j th scatterer in the presence of other scatterers.

It is interesting to compare (150) with the usually ladder approximation. In the usual ladder approximation, the second term in (150) is absent and secondly the $\overline{\overline{\widehat{C}}}_l$ in (150) is replaced by $\overline{\overline{T}}_l$ which is the transition matrix of the l th particle in the absence of other scatterers. Obviously, the two cases reduce to each other for sparse concentration

of particles when $n_{s_j} n_{s_l} h_{s_j s_l}$ can be neglected and $\overline{\overline{\hat{C}}}_l$ is approximately equal to $\overline{\overline{T}}_l$. Equation (150) is also the intensity operator under ladder approximation for multiple species which will be useful for second moment calculations.

3.7 Conclusion

In this chapter, we have studied the problem of effective propagation constants in media with densely distributed dielectric particles of multiple sizes and permittivities. The problem is complicated by the fact that for high concentrations of particles, the particles do not scatter independently. In this chapter, we have employed QCA and QCA–CP approximations to calculate the effective propagation constants incorporating the effect of correlated scatterers. The imaginary part of the complex effective propagation constant gives the attenuation rate of the coherent wave due to both scattering and absorption. The particles in natural geophysical terrain usually follow a drop size distribution which can be discretized and represented by a histogram. The approach described in this paper can find useful applications to such problems of random discrete scatterers of multiple sizes. It also finds applications to problems of random discrete scatterers of multiple permittivities in geophysical terrain and composite materials.

The results of the effective propagation constants under QCA and QCA–CP depend on the pair distribution functions of particle positions. In this chapter, the pair distribution functions of non-interpenetrable spheres of multiple sizes are calculated by the Percus–Yevick approximation.

For the case of small particles, analytic closed form expressions are derived for the effective propagation constants under QCA and QCA–CP. The effective propagation constants for moderate size particles under QCA are solved by numerical techniques.

For problems of lossless particles or slightly lossy particles, it is also important to calculate the second moment of the incoherent fields. A common approximation for the Bethe–Salpeter second moment equation is the ladder approximation which can include the effect of correlated scattering through the pair distribution function as discussed in section 3.6. It is also seen in section 3.6 that the QCA–CP is consistent with the ladder approximation in that the integrated

optical relation is satisfied. The ladder approximation has been used in conjunction with QCA–CP to derive a set of dense media radiative transfer equations that includes the effect of correlated scatterers.

Finally, we will mention a few other approaches that have been used to calculate the effective propagation constants in dense media. The strong permittivity fluctuation approach uses the bilocal approximation of continuous random medium theory and takes into account the singularity of the dyadic Green's function [8,35–37]. The effective medium approximation consisting of a set of coupled integral equations for the effective T-matrix and effective distribution functions has also been used [9,38–41]. The QCA approximation has been used to consider the case of nonspherical particles [42]. Monte Carlo calculations have also been made on the pair distribution function of aligned identical spheroidal particles [43].

References

[1] Twersky, V., "Coherent scalar field in pair-correlated random distributions of aligned scatterers," *J. Math. Phys.*, **18**, 2468–2486, 1977.

[2] Tsang, L. and J. A. Kong, "Multiple scattering of electromagnetic waves by random distribution of discrete scatterers with coherent potential and quantum mechanical formulism," *J. Appl. Phys.*, **15**, 3465–3485, 1980.

[3] Tsang, L., J. A. Kong, and T. Habashy, "Multiple scattering of acoustic waves by random distribution of discrete spherical scatterers with the quasi-crystalline and Percus-Yevick approximation," *J. Acoust. Soc. Am.*, **71**, 552–558, 1982.

[4] Tsang, L. and J. A. Kong, "Effective propagation constants for coherent electromagnetic wave propagation in media embedded with dielectric scatterers," *J. Appl. Phys.*, **53**, 7162–7173, 1982.

[5] Ishimaru, A. and Y. Kuga, "Attenuation constant of a coherent field in a dense distribution of particles,," *J. Opt. Soc. Am.*, **72**, 1317–1320, 1982.

[6] Tsang, L. and J. A. Kong, "Scattering of electromagnetic waves

from a half space of densely distributed dielectric scatterers," *Radio Science,* **18,** 1260–1272, 1983.

[7] Varadan, V. K., V. N. Bringi, V. V. Varadan, and A. Ishimaru, "Multiple scattering theory for waves in discrete random media and comparison with experiments," *Radio Science,* **18,** 321–327, 1983.

[8] Tsang, L., J. A. Kong, and R. T. Shin, *Theory of Microwave Remote Sensing,* Wiley-Interscience, New York, 1985.

[9] Zhu, P. A., A. K. Fung, and K. W. Wong, "Effective propagation constants in dense random media under effective medium approximation," *Radio Science,* **22,** 234–250, 1987.

[10] Wertheim, M. S., "Exact solution of the Percus-Yevick integral equation for hard spheres," *Phys. Rev. Lett.,* **20,** 321–323, 1963.

[11] Lebowitz, J. L., "Exact solution of generalized Percus-Yevick equation for a mixture of hard spheres," *Phys. Rev.,* **133,** A895–899, 1964.

[12] Wertheim, M. S., "Analytic solution of the Percus-Yevick equation," *J. Math. Phys.,* **5,** 643–651, 1964.

[13] Baxter, R. J., "Ornstein-Zernike relation for a disordered fluid," *Aust. J. Phys.,* **21,** 563–569, 1968.

[14] Baxter, R. J., "Ornstein-Zernike relation and Percus-Yevick approximation for fluid mixtures," *J. Chem. Phys.,* **52,** 4559–4562, 1970.

[15] Leonard, P. J., D. Henderson, and J. A. Barker, "Calculation of the radial distribution function of hard-sphere mixtures in the Percus-Yevick approximation," *Molec. Phys.,* **21,** 107–111, 1971.

[16] Waseda, Y., *The Structure of Non-Crystalline Materials, Liquids and Amorphous Solids,* McGraw-Hill, New York, 1980.

[17] Frisch, V., "Wave propagation in random medium," in *Probabilistic Methods in Applied Mathematics,* A. T. Bharucha-Reid, ed., Academic Press, New York, 1968.

[18] Ishimaru, A., *Wave Propagation and Scattering in Random Media,* **1 , 2,** Academic Press, New York, 1978.

[19] Tatarskii, V. I., *The Effects of Turbulent Atmosphere on Wave Propagation,* National Technical Information Service, Springfield,

Va., 1971.

[20] Tsang, L. and A. Ishimaru, "Radiative wave and cyclical transfer equation for dense nontenuous media," *J. Opt. Soc. Am. A*, **2**, 2187–2194, 1985.

[21] Tsang, L. and A. Ishimaru, "Radiative wave equations for vector electromagnetic propagation in dense nontenuous media," *J. of Electromagnetic Waves and Applications*, **1**, 59–72, 1987.

[22] Tsang, L., "Passive remote sensing of dense nontenuous media," *J. of Electromagnetic Waves and Applications*, **1**, 159–173, 1987.

[23] Soven, P., "Coherent-potential model of substitutional disordered alloys," *Phys. Rev.*, **156**, 809–813, 1967.

[24] Gyorffy, B. L., "Electronic states in liquid metals: A generalization of the coherent–potential approximation for a system with short-range order," *Phys. Rev. B.*, **1**, 3290–3299, 1970.

[25] Korringa, J. and R. L. Mills, "Coherent potential approximation for random systems with short range correlations," *Phys. Rev. B.*, **5**, 1654–1655, 1972.

[26] Kohler, W. E. and G. C. Papanicolaou, "Some applications of the coherent potential approximation," in *Multiple Scattering and Waves in Random Media*, P. L. Chow, W. K. Kohler and G. C. Papanicolaou, eds., North-Holland, New York, 199–223, 1981.

[27] Schanda, E., "Microwave modelling of snow and soil," *J. of Electromagnetic Waves and Applications*, **1**, 1–24, 1987.

[28] Hallikainen, M. T., F. T. Ulaby, and T. E. Van Deventer, "Extinction behavior of dry snow in the 18-90 GHz range," *IEEE Trans. Geosci. Remote Sensing*, **GE-25**, 737–745, 1987.

[29] Rayleigh, L., "On the influence of obstacles arranged in rectangular order on the properties of a medium," *Phil. Mag.*, **34**, 481–502, 1892.

[30] Tai, C. T., *Dyadic Green's Function in Electromagnetic Theory*, International Textbook, Scranton, PA., 1971.

[31] Cruzan, O. R., "Translational addition theorems for spherical vector wave functions," TR–906, Diamond Ordinance Fuse Laboratories, Department of the Army, Washington DC., 1961.

[32] Cruzan, O. R., "Translational addition theorems for spherical vec-

tor wave functions," *Quart. J. Appl. Math.*, **20**, 33–40, 1962.

[33] Edmonds, A. R., *Angular Momentum in Quantum Mechanics*, Princeton University, Princeton, NJ., 1957.

[34] Born, M. and E. Wolf, *Principles of Optics*, fifth edition, Pergamon, New York, 1975.

[35] Tsang, L. and J. A. Kong, "Scattering of electromagnetic waves from random media with strong permittivity fluctuations," *Radio Science*, **16**, 303–320, 1981.

[36] Tsang, L., J. A. Kong, and R. W. Newton, "Application of strong fluctuation random medium theory to scattering of electromagnetic waves from a half space of dielectric mixture," *IEEE Trans. Ant. Prop.*, **AP-30**, 292–302, 1982.

[37] Stogryn, A., "Correlation functions for random granular media in strong fluctuation theory," *IEEE Trans. Geosci. Remote Sensing*, **GE-22**, 150–154, 1984.

[38] Roth, L., "Effective medium approximation for liquid metals," *Phys. Rev. B.*, **4**, 2476–2484, 1974.

[39] Singh, V. A., "Analytic unitary preserving approximations for the electronic structure of amorphous systems," *Phys. Rev. B.*, **24**, 4852–4854, 1981.

[40] Schwartz, L. and T. J. Plona, "Ultrasonic propagation in closed-packaged disordered suspensions," *J. Appl. Phys.*, **55**, 3971–3977, 1984.

[41] Davis, V. A. and L. Schwartz, "Electromagnetic propagation in close-packed disordered suspensions," *Phys. Rev. B.*, **31**, 5155–5165, 1985.

[42] Tsang, L., "Scattering of electromagnetic waves from a half space of nonspherical particles," *Radio Science*, **19**, 1450–1460, 1984.

[43] Varadan, V. V., V. K. Varadan, Y. Ma, and W. A. Steele, "Effects of nonspherical statistics on EM wave propagation in discrete random media," *Radio Science*, **22**, 491–498, 1987.